EXPLORING IMAGING TECHNOLOGY IN THE DIAGNOSIS AND TREATMENT OF

PEDIATRIC MEDICALLY REFRACTORY EPILEPSY

WITH INTRACRANIAL ELECTROENCEPHALOGRAPHY AND POST-SURGICAL EVALUATIONS

By

Nasheha Baset

Presented to the Faculty of the Graduate School of

The University of Texas at Arlington

In Partial Fulfillment of the Requirements for the Degree of

MASTER OF SCIENCE IN BIOMEDICAL ENGINEERING

THE UNIVERSITY OF TEXAS AT ARLINGTON

MAY 2021

Supervising Committee:

Dr. Christos Papadelis, Supervising Professor

Dr. George Alexandrakis

Dr. Hanli Liu

Abstract

Exploring Imaging Technology in the Diagnosis and Treatment of Pediatric Medically Refractory Epilepsy

with Intracranial Electroencephalography and Post-Surgical Evaluations

Nasheha Baset, MS

The University of Texas at Arlington, May 2021

Supervising Professor: Dr. Christos Papadelis

Epilepsy is a disorder that commonly causes seizures due to abnormal neurological activity, which can disrupt daily life. Of all patients with epilepsy, 60% suffer from focal epilepsy. Approximately 15% of these cases are considered to be drug resistant, or refractory, as the patient is not responsive to a combination of two or more anti-epileptic drugs (AED). Traditionally, approaches to treatment of medically refractory epilepsy include lobotomies, resections, or surgical severing of nerves in the cortex, in order to achieve seizure freedom. These risks include, but are not limited to, higher risk of infection due to its invasive nature, possible consequences of changes to their personality, and possible changes to their intellectual functions. For this reason, laser ablations are becoming more popular as they greatly reduce discomforts, recovery time, and morbidity being greatly reduced compared to traditional resections.

Children are different than their adult counterparts in that seizure frequency typically tends to be higher in children than adults, and that the child's brain is very neuroplastic and reorganizing as they grow. The Seizure Onset Zone (SOZ) is the area also in the cortex where the epileptiform discharges are generated when localized by a scalp or intracranial electroencephalogram (iEEG). The Resection Zone (RZ) is the region that resected or ablated during surgery to optimally reduce seizure occurrence. The Epileptogenic Zone (EZ) is the minimum area of the cortex that would need to be resected or ablated to allow for seizure freedom. IEEG, or intracranial electroencephalogram, measures the electric potential directly from the brain's surface using electrocorticography (ECOG) electrodes and stereotactic EEG

(SEEG). Functional connectivity (FC) is defined as the study of temporal connections between spatially distinct neurophysiological events.

To evaluate the efficacy of the laser ablation procedure, we retrospectively analyzed the medical records from 36 children with medically refractory epilepsy who have undergone epilepsy surgery with laser ablation at Cook Children's Health Care System. We examined the surgical outcome of the patients by their post-surgery Engel scores and the number of AEDs, and conducted t-tests to evaluate differences.

To develop the interictal functional connectivity biomarker of the Epileptogenic Zone, we analyzed iEEG data from 19 patients with medically refractory epilepsy undergone resective surgery (13 with good surgical outcome and 6 with poor surgical outcome) from Boston Children's Hospital. We filtered the iEEG data in the following frequency bands: 1-70 Hz for spikes, and 80-250 Hz for ripples, and both 1-70 Hz and 80-250 Hz for simultaneous spike and ripple events. Then, we estimated the following functional connectivity matrixes: AEC, PLV, and CORR. We compared these functional connectivity measures for electrodes inside the Seizure Onset Zone and the Resection Zone and performed statistical analysis between these measures using Wilcoxon signed-rank test.

Due to the small cohort for the evaluation of AEDs before the laser ablation study, many tests did not meet the requirements to be run, and for the tests that did meet the requirements, significant results were not found in all, but one test (p-value = 0.000574, α = 0.05). For the functional connectivity study using iEEG data to identify the Epileptogenic Zone, significant results were not found in all, but two of the tests, first when comparing the inside and the outside regions of the Seizure Onset Zone in poor outcome patients using CORR (80-250Hz) (p-value = 0.03125, α = 0.05) and comparing the inside to the outside regions of the Resection Zone in good outcome patients using CORR (1-70 Hz) (p-value = 0.03979, α = 0.05). These results do not support the current literature, leading to the conclusion that expanding the cohort of the AED and ablation study, and reevaluating the methodology of the functional connectivity of the Epileptogenic Zone study will not only open more doors as to how we can improve the localization of epilepsy, but also provide a better understanding of the diagnoses and treatment of this disease as well. Although we rejected our initial hypothesis, we now know that there is great promise in modifying and continuing these studies long term.

Acknowledgements

Dedication

To my loving parents, Nahid and Nasir Baset, and my sisters Neshat, Saiyara, and Safia Baset, who have

all managed to keep me sane the last two years. I wouldn't have been able to do it without you. To God

for listening to my prayers in times of frustration.

I love you and thank you.

Table of Contents

List of Figures

List of Tables

CHAPTER 1

INTRODUCTION

1.1 What is Epilepsy?:

Defined by the International League Against Epilepsy (ILAE) in 2014, epilepsy is a disease of the brain defined by any of the three conditions: 1) At least two unprovoked, or reflex, seizures occurring >24 hours apart, 2) One unprovoked, or reflex, seizure and a probability of further seizures similar to the general recurrence risk (at least 60%) after two unprovoked seizures, occurring over the next 10 years, or 3) Diagnosis of an epilepsy syndrome [1]."

The ILAE further explains that epilepsy can be declared and considered to be resolved if the patient had an age-dependent epilepsy syndrome, are past the age that the syndrome would have occurred, have not experienced seizures within the last 10 years, and have not experienced seizures while not on medication for the last 5 years [1]. Oftentimes, scales and classifications, similar to the one in the table 1 below, are used to further describe the progression or recovery of the disease post-surgery.

Table 1. Description of the Engel Outcome Classifications

ILAE Engel Outcome Scale and Classification	Description
Class 1	Completely seizure free; no auras
Class 1a*	Completely seizure free since surgery; no auras
Class 2	Only auras; no other seizures
Class 3	1-3 seizure days per year ± auras
Class 4	Four seizure days per year to 50% reduction of baseline seizure days; ± auras
Class 5	<50% reduction of baseline seizure days to 100% increase of baseline seizure days; ± auras
Class 6	>100% increase of baseline seizure days

Condensed Engel Scale, used to evaluate the reduction or worsening of symptoms and frequency of symptoms for epilepsy. *Differentiates from Class 1, which refers to seizure freedom within the last year of follow-up.

Epileptic seizures can range from being undetectable and only identified when using medical imaging, to longer episodes that have outward symptoms, like laughter, shaking, and unresponsiveness to name a few. Due to these varied symptoms, it can disturb the patient's normal daily life, social interactions,

and activities, and possibly cause them to be victims of stigma, whether that be institutional, interpersonal, or internalized [2].

Many times, these seizures may not have an outward reason or cause, although sometimes it may be caused by traumatic brain injury, brain malformation, or other physical or chemical differences of the brain. Isolated instances of seizures are not considered to be a part of epilepsy, for example, an allergy to a food or medication [1], and formal diagnosis is required by a medical professional.

It was found in 2015 that approximately 1.2% of the U.S. population reported being actively diagnosed with epilepsy; this includes 3 million adults and 470,000 children, for a total of 3.4 million people, with the number found to continue to grow as the population grows [3]. From these surveys, it was found that 0.6% of children between the ages of 0-17 years have active epilepsy [3, 4]. Epilepsy was found to be more prevalent in older, male children from lower income families. Children diagnosed with epilepsy were found to experience higher rates of developmental, behavioral, and mental health disorders including depression (8% in children diagnosed with epilepsy vs 2% in healthy children), anxiety (17% vs 3%), autism spectrum disorder (16% vs 1%), and developmental delay (51% vs 3%) to name a few [4]. It is due to these demographics and stigmas that it is crucial that higher quality and safer treatment is provided to those experiencing epilepsy, as it will help lead to a more normalized life.

1.2 How Pediatric Refractory Epilepsy is Different:

In 1981, the ILAE categorized and classified epileptic seizure events into three main categories: partial, generalized, and unclassified. There are subcategories within these three categories as well that help describe the type of event, like focal, clonic, or tonic. A requirement to categorize these events is to take an electroencephalogram (EEG) recording of the patient, between and/or during events. In many cases, epilepsy could be due to structural abnormalities, which can be seen in Computer Tomography (CT) scans or Magnetic Resonance Imaging (MRI) scans [5]. We present here examples of patients with medically refractory epilepsy with abnormal MRIs during pre-procedure imaging. In figure 1A and 1B, we see a patient from the intracranial encephalography study, later described in this paper, with a structural abnormality, specifically an asymmetry where the left temporal lobe is smaller than the right. Figure 2A and 2B shows an example of a T1 weighted image and post-procedure fluid attenuated inversion recovery (FLAIR) image of a child with Focal Cortical Dysplasia [6]. In figure 3A and 3B, we see an example of another T1 and

FLAIR image of a healthy patient without malformations for comparison [7]. Figures 1 and 2 are a few examples of possible structural abnormalities that can cause refractory epilepsy in children. T1 weighted images and FLAIR images are created using different sequences or magnetic gradients of MRIs [7]. In sections 1.4 and 1.5, we further explore and describe MRI (T1 and FLAIR), EEG, CT, and other imaging technologies to better understand their role in diagnosis and treatment of this disease.
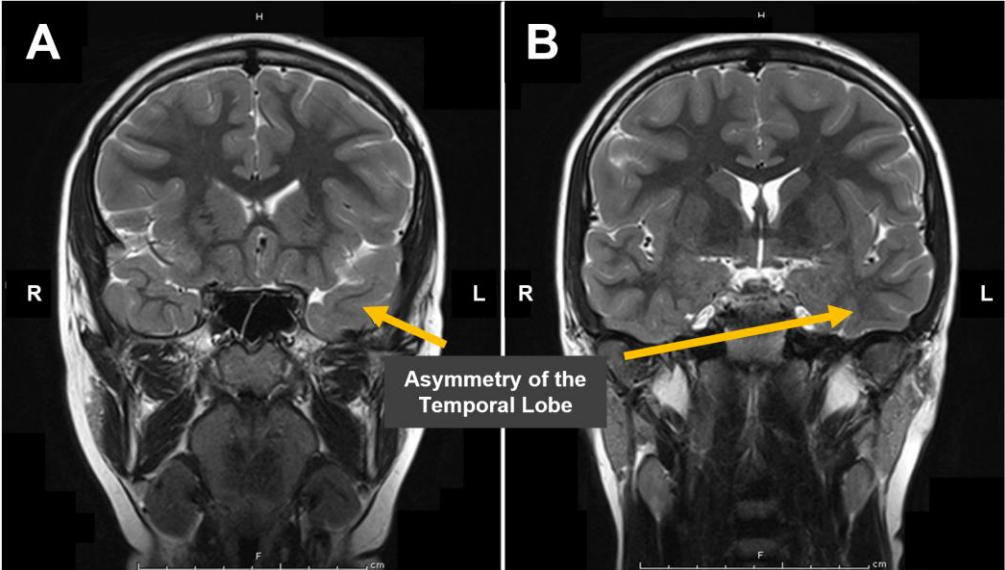
Figure 1. MRI of a 12 year old patient from the intracranial electroencephalography study, later described in this paper, with a smaller left temporal lobe than the right; A) arrow points to the asymmetry located in the left area of the temporal lobe; B) another MRI slice of the same asymmetry.
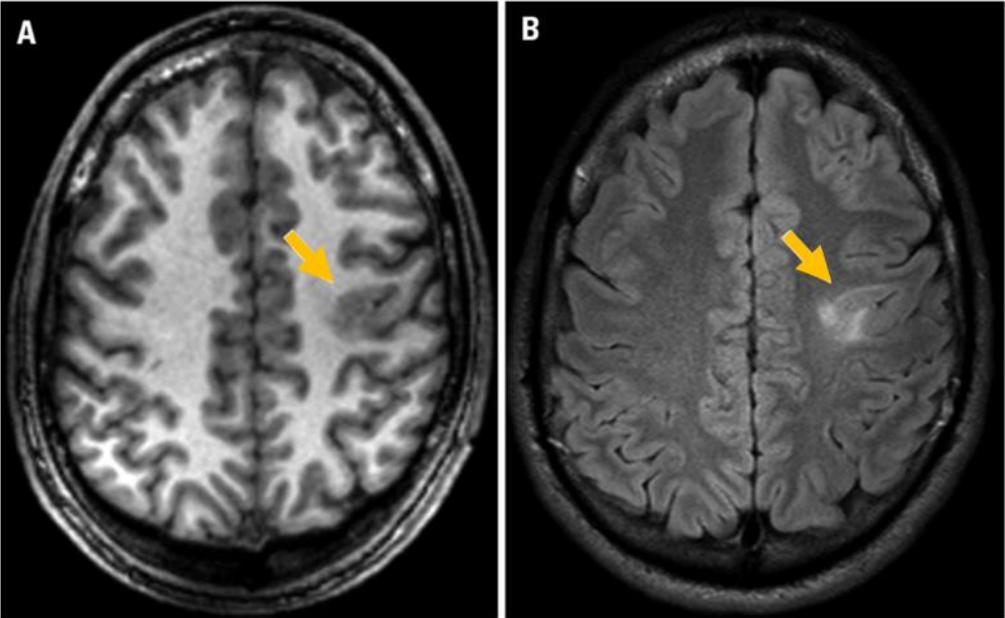
Figure 2. A) MRI scan of a patient with focal cortical dysplasia (T1 weighted), and B) FLAIR image of the same patient; the arrows indicate the area of question, specifically the area of mild cortical thickening [6].
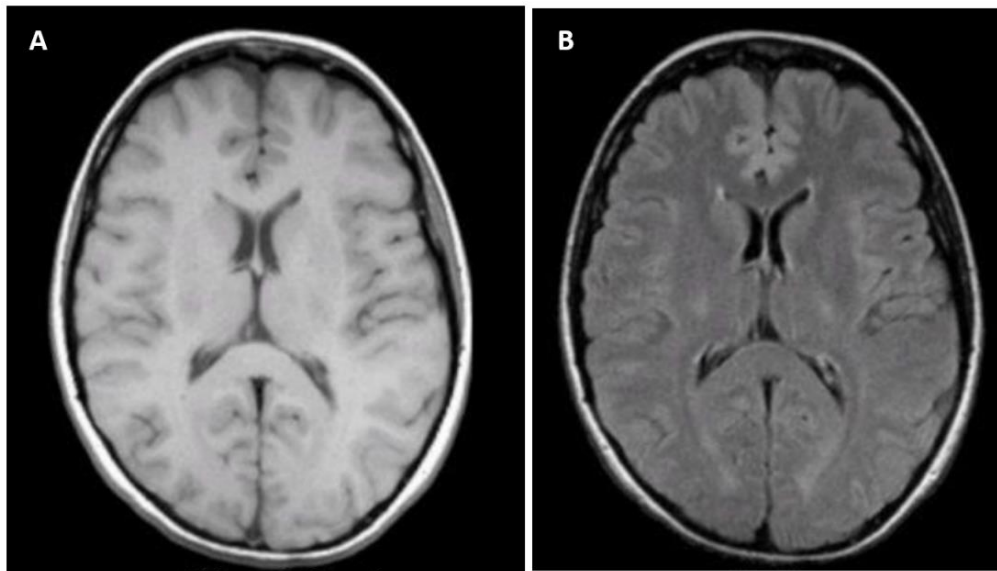
Figure 3. A) MRI scan of a patient with a healthy brain (T1 weighted), and B) FLAIR image of the same patient [7].

Of all patients with epilepsy, 60% suffer from focal epilepsy. Approximately 15% of these cases are considered to be drug resistant, or refractory, as the patient is not responsive to a combination of two or more of these anti-epileptic drugs (AED) [8]. After they are categorized as treatment, or drug resistant, and they do not respond to treatments involving the vagal nerve stimulation (only available in children above the age of 12) [9], and diet changes, like the ketogenic diet, surgical intervention is warranted. Traditionally, these surgeries are lobotomies, resections, or surgical severing of nerves in the prefrontal lobe of the brain, in order to achieve seizure freedom. Along with the major possible benefit of a procedure as a lobotomy to gain the seizure freedom, there are risks. These risks include, but are not limited to, higher risk of infection due to its invasive nature, possible consequences of changes to their personality, and possible changes to their intellectual functions [10].

Children are different than their adult counterparts in that seizure frequency typically tends to be higher in children than adults, and that the child's brain is very neuroplastic and reorganizing as they grow [11, 12]. In children younger than 2 years of age, seizures are likely associated with developmental delays; dysplasia is often more common in children than adults, and focal epilepsy present in childhood is often due to age-specific etiology [11, 12, 13]. In certain neurological disorders, like epilepsy, being able to conduct a brain procedure on those that are AED resistant can possibly allow for greater likelihood of

achieving homeostasis in adulthood than adults who undergo the same procedure; this is likely due to neuroplasticity that is still ongoing in childhood [14]. Meaning if surgical intervention is done early enough after it is determined that the quality of life may likely improve after surgery, doing it during earlier in the childhood years allows for a greater chance of allowing the patient to slowly continue on to a more normal life, due to the initial overproduction of nerves during infancy and deletion of synapses and neurons with age, and overall stabilization of those synapses; brain injury, neurological disorders or imbalances, or interventions can alter the way the these deletions are done or not done by the brain [15].

1.3 Zones and Areas of the Cortex:

The rise for the need of differentiating zones and areas of the cortex was accelerated as imaging technologies allowed for better visualizations of the brain, especially when it came to resective surgeries for severe cases. Resective surgery depends on accurate delineations of the Epileptogenic Zone in individual patients, as well as operative zones, functional zones, and the onset zones, for successful and complete resection to occur [16]. Slight structural and operative differences between patients meant that these zones need to be tailored to the individual patients.

In the late 1800s and early 1900s, surgeries for epilepsy were highly discouraged due to the high rates of death and serious brain damage as a result of not having the tools available to visualize the brain structures, zones, and areas. In 1934, the invention of the "Montreal Procedure" for surgical treatment of epilepsy was developed to remove the Epileptogenic Zone. This involved removing a section of the skull of a conscious epileptic patient to expose the cortex, using probes to identify the Epileptogenic Zone by having the patient verbalize their feelings and experiences when the area is probed by the surgeon, and finally the surgeon estimating and resecting the Epileptogenic Zone without disturbing any of the other eloquent or functional zones [17, 18].

The creation and implementation of the electroencephalogram (EEG) was a major turning point in the development of surgical techniques for epilepsy, specifically in defining zones and areas of the brain, which was first employed and documented as use for temporal lobe surgery in 1951 [18, 19]. Surgeons and medical professionals began to define these zones more accurately in patients, reducing the risk of these surgeries, while also gaining more knowledge and understanding of the structure and organization of the cortex. In the past 70 years, imaging technologies such as magnetic resonance imaging (MRI) and

computed tomography (CT), as well as invasive subdural recordings like electrocorticography (ECOG) and stereo encephalography (SEEG), revolutionized the accuracy of estimations of these areas and zones, allowing for an increase in the post-operative outcome for seizure freedom (further described in section 1.4) [16, 18]. This also preserves areas that are crucial for motor, language, sensory, and somatosensory functions, to name a few. Below is a list of these zones and areas:

- The **Symptomatogenic Zone** is the part of the cortex that becomes activated by the epileptiform discharge, producing the symptoms that occur during the seizure, or ictal symptoms [8].

- The **Irritative Zone** has been defined as the region of the cortex that generates the interictal, or between seizure, electrographic spikes [8].

- The **Epileptogenic Zone** (EZ) is the minimum area of the cortex that would need to be resected or ablated to allow for seizure freedom [8, 20]. Many times, this includes a known region and a potential region, but there is currently no diagnostic method of isolating and visualizing this region [8].

- The **Resection Zone** (RZ) is the region of area that is determined to be the Seizure Onset Zone, that is then resected or ablated during surgery to optimally reduce seizure occurrence [8].

- The **Functional Deficit Zone** is the region in the cortex that is "functionally abnormal in the interictal period", whether this is due to the lesion created or a pre-existing abnormality [8].

- The **Seizure Onset Zone** (SOZ) is the area also in the cortex where the epileptiform discharges are generated when localized by a scalp or iEEG [8].

- The **Primary Motor Cortex** is an area of the cortex where when electrical stimulation is applied, it evokes movement in the peripheral nervous system areas, first seen my Hitzig and Fritsch [21, 22].

- The **Somatosensory Area** is the area of the brain that carries information about the state of the body and how it is physically interacting and the information it gathers about its surrounding environment [23].

- The **Eloquent Cortex** is the area of the brain that is necessary for sensory processing and linguistic ability. This includes regions such as the left temporal and frontal lobes for language and speech, the occipital lobes for vision, parietal lobes for sensation, the primary motor cortex for movement, and the somatosensory area for the processing of sensory information. These areas can be seen

in figure 4 below. Removal of these eloquent areas may cause sensory loss, language loss, or

possible paralysis [24]. These areas are taken into consideration when surgical planning occurs.

In figure 4, we see an illustration of these zones, with respect to other primary areas and zones, like the

language, motor, and visual areas, that might possibly overlap or have a connecting effect.
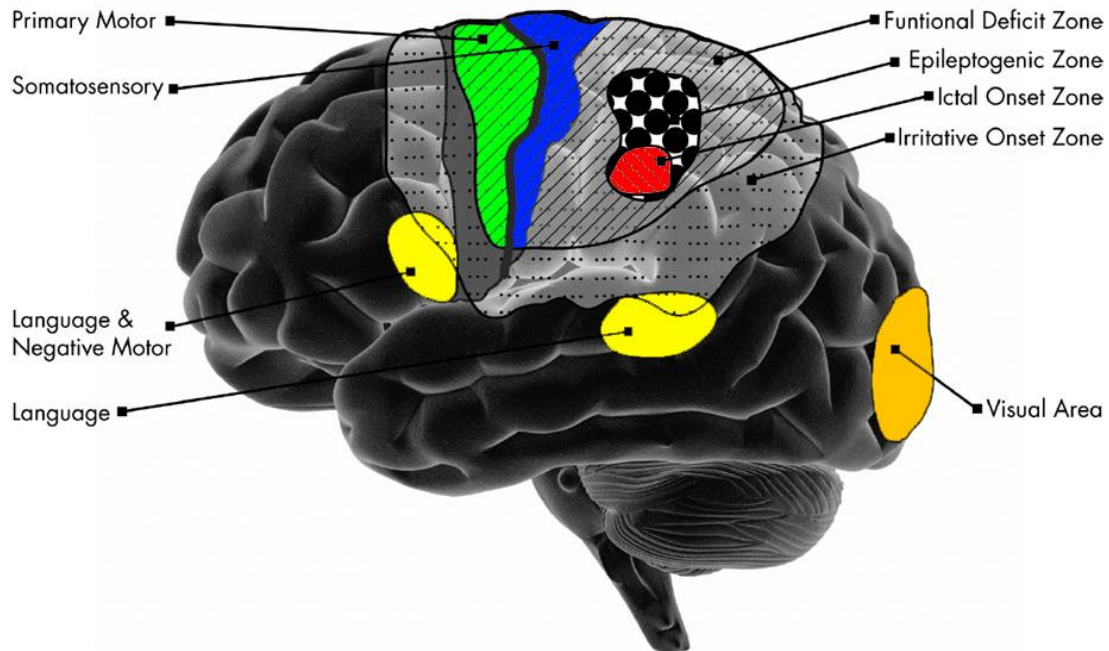
Figure 4. Zones and areas of interest for epilepsy when evaluating, understanding, and visualizing the cortex of the brain [16].

1.4 EEG, iEEG, ECOG, SEEG, and MRI:

EEG, or electroencephalogram, is the most widely and commonly used imaging technique when diagnosing

pediatric epilepsy [25, 26]. This is due to its ability to record unusual activity relatively well and accurately,

while also being readily accessible and affordable. It is typically non-invasive, and it measures the

coordinated action potentials, or spikes, over time that are detected from the neurons in the brain [25, 26,

27]. The brain produces oscillations during a normal state, and any deviation from it could indicate a

potential problem [27]. Prolonged EEGs may be recorded, even multiple day video EEGs, in order to get

accurate ictal and interictal recordings to evaluate.

iEEG, or intracranial electroencephalogram (also referred to as icEEG; figure 5), measures the

electric potential directly from the brain's surface using electrocorticography (ECOG) electrodes [28], seen

in the center image of figure 5. The electrodes are placed under the skull on the brain above the region

where epileptogenic activity is estimated to occur [29, 30]. Usually, the arrangement of ECOG electrodes is either in strips or grids, connected to wires that exit the head, which are connected to an amplifier that is used to record EEG signals from each implanted strip or grid, and are most commonly used when the area of interest can be measured from the surface of the cortex [29, 30, 31].
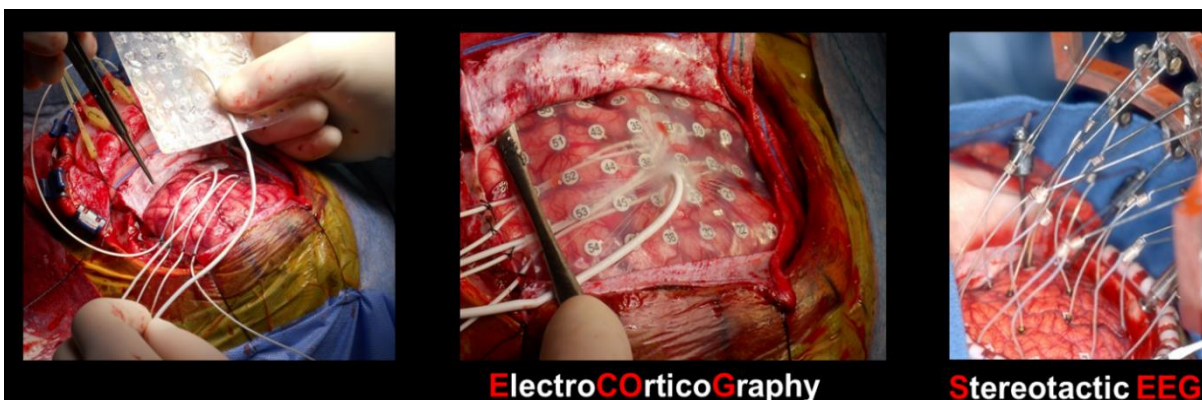
Figure 5. Images from ECOG and SEEG implantation, with grid placement in the middle image, ECOG, and depth electrodes in the far right image, SEEG (Courtesy of Dr. Christos Papadelis).

SEEG, or stereotactic EEG, is different than an ECOG, as it requires burr holes to implant what is commonly called a depth electrode into the patient's brain [30, 32], as seen in the right image of figure 5. This can be inserted in many different configurations in several lobes, like the occipital or the hippocampus, and works best to collect recordings from structures deeper in the brain [30, 32]; it is most often used when monitoring areas of the cortex that may not be directly measured from the surface. A common disadvantage of this is that it covers less area than the ECOG, but is customizable to collect measurements from the desired locations. It is an excellent technique to understand and localize the Epileptogenic Zones in patients with refractory epilepsy, and with recent developments like using robotic-guided stereotactic EEG for SEEG electrode placement, similar to what will be seen in figure 7 of section 1.5, this procedure is now considered very safe as regular procedure for evaluation [32, 33].

MRI, magnetic resonance imaging, is an imaging technique used to detect any possible anatomical abnormalities that may be the cause of the epilepsy [34]. This is commonly seen as the technique used when diagnosing focal cortical dysplasia or hippocampal sclerosis, similarly described in chapter 3, by epileptologists in order to cater the care and to the patient's unique needs [35, 36]. It is highly sensitive and allows for exceptional tissue contrast for evaluation [34]. Two types of commonly used MRI sequences are

T1 weighted images and FLAIR images, which are created using different magnetic gradients of the MRIs [7].

With recordings from EEG and iEEG (i.e., ECOG and SEEG), the goal is to collect two types of activity, ictal and interictal in order to better localize the Epileptogenic Zone. Ictal is the critical detected activity during the occurrence of a seizure, frequently seen as consistent patterns of waves or spikes. Interictal activity are the spikes, ripples, waves, and other activity seen when clinical seizures are not occurring [37]. Many times, spikes (further explained in section 1.7) are seen during these events, as pictured in the far right image in figure 6 during interictal activity.
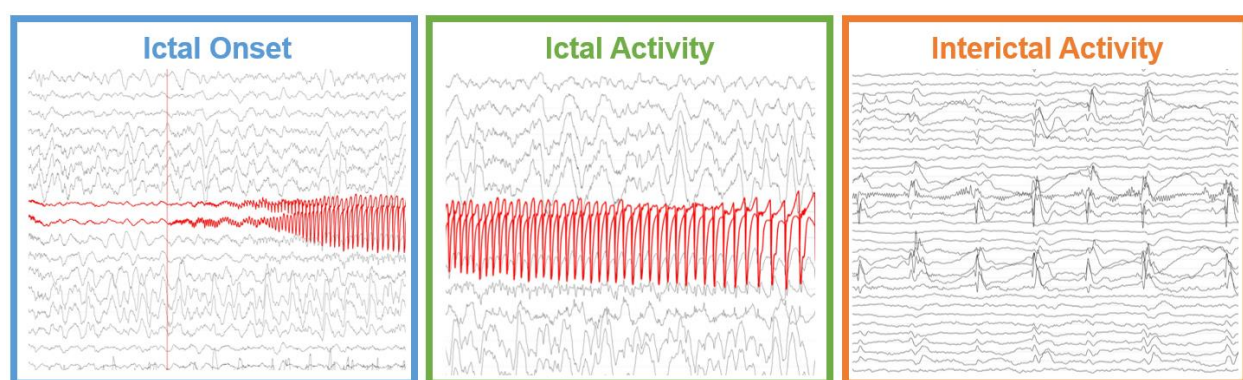
Figure 6. IEEG recording of a tonic clonic patient from the intracranial electroencephalography study, later described in this paper, with the left image showing the ictal onset with the vertical red line signifying the point of onset, the middle image shows ictal (during seizures), and the right image showing interictal (between seizures) activity. The red coloring is for easier visualization of the activity.

1.5 Traditional Lobotomies and Resections versus Robotic-Guided Stereotactic Laser Ablations:

Since 1965, the use of lasers in Neurosurgery have been explored, the first of which was extremely informative, but highly unsuccessful [38, 39]. Over the past 56 years, learning to control the heat and intensity of the laser, as well as combining on demand imaging technologies and using the assistance of a robotic arm (commercially referred to as robotic-guided stereotactic EEG laser ablation, or ROSA), has helped to greatly improve the precision and accuracy of this procedure, so much so that it is favored to help gain control of many cases of refractory epilepsy, especially in children [40], similar to what is seen in figure 7 where it's being used for stereo electroencephalography (SEEG) electrode placement, which is one application of robotic-guided stereotactic EEG. A few of these imaging technologies involved in this procedure are T1 weighted images and post-procedure fluid attenuated inversion recovery (FLAIR) are MRI sequences at different magnetic gradients that create visuals of the brain by displaying bright or dark areas

using information gathered from the properties found in fluid flow, fat content, and tissue density [7]. Computerized Tomography scan (CT) combines X-ray images from different angles to create cross section images of soft tissue, blood vessels, and bones for better visualization and accurate implantation of SEEG electrodes or probe placement [41]. With current advancements, the images can be produced quickly and easily during the procedure for a more accurate and effective treatment.

Figure 7. The Robotic-Guided Stereotactic EEG (ROSA) arm placed in the "home" setting after precise placement of SEEG electrodes [42].

By using laser ablation, the procedure is significantly less invasive which reduces the area to a few burr holes. It also reduces the procedure time due to the robotic assistance. The few burr holes cuts the duration of the hospital stay to usually no more than two days, allowing for quicker overall recovery time which helps the patient to resume normal life more rapidly, and infection control is a lot more manageable. The laser ablation that is described in this paper, has been developed over many years and approved by the FDA as a highly safe and effective surgical laser ablation system. The robotic-guided stereotactic EEG system is also referred to as MRI-guided laser interstitial thermal therapy (MRgLITT), Visualase Thermal Therapy System (manufactured by Visualase, Inc.), or commercially as ROSA.

Before the procedure is conducted, presurgical evaluations are done in order to determine if this is the correct approach for the patient. For this, a team of epilepsy specialists evaluate the patient, their medical histories, as well as any imaging that may give a clear picture as to if the procedure is appropriate, and if so, how surgical planning must be done in order to have the most successful procedure. These can

be MRI scans, like the T1 and FLAIR images previously mentioned, CT scans for structural abnormality detection, video EEGs which is an electroencephalogram that is simultaneously recorded with a video of the patient's symptoms over a duration of time [43], and SEEG recordings which stereotactic EEG which collect recordings of activity from structures deeper in the brain [30, 32], to name a few.

The robot-guided stereotactic EEG robotic arm is connected to an image processing station, figure 8, that provides real time MRI imaging and heat maps during surgery, with a compatible 15 W, 980-nm diode laser and peristaltic pump connected to a cooled laser applicator, which is approximately 1.65 mm in diameter and has a 400μm core silica fiber optic applicator and a light diffusing tip as seen in figure 9B. The outer layer is comprised of a flexible and light transmissive cooling sheath.

Figure 8. A) Visualase workstation without the arm, with two monitors, the peristaltic pump for the coolant on the bottom level of the station to the left, and the diode laser to the right to the right. B) A screen shot of the top monitor while the bottom monitor allows you to toggle between images and viewpoints, C) a closeup of the heat map in real time of the top monitor with the irreversible damage zone versus ablation zone [44].
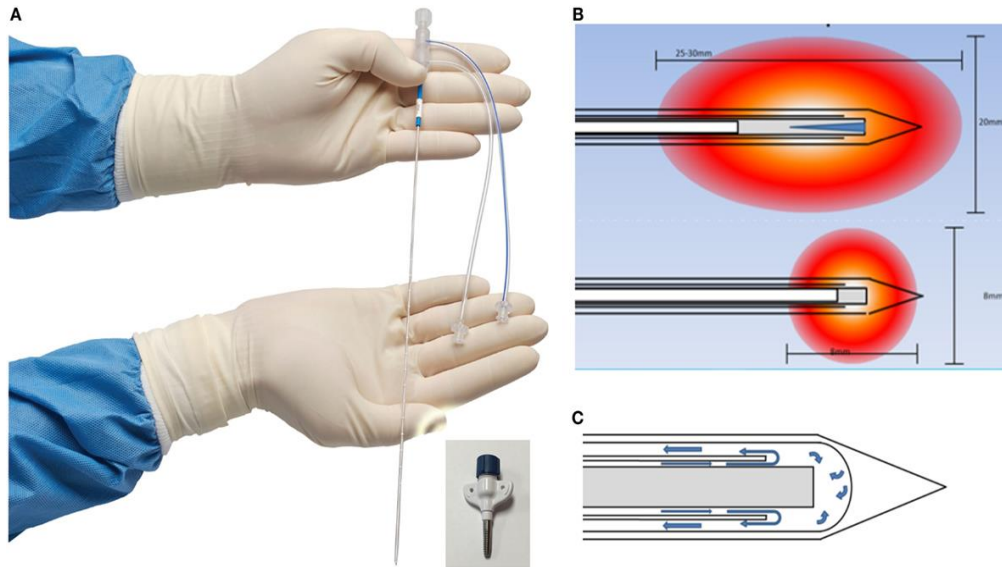
Figure 9. A) A cooled laser applicator with one port for the inflow of saline coolant, and another port for the outflow of the coolant. The anchor is pictured as the small image in the bottom center. B) Visualase probe with 10mm (top) and 3mm (bottom) diffuser tips, with the red and yellow being the simulated region of ablation. C) Depiction of the coolant flow in the probe's two channel system [45, 46].

The light that it produces is roughly in an ellipsoid to cylindrical shape distribution along the 1 cm diffusing element, which is the axis [40, 47, 48], which is seen in the top image of figure 9B. The bottom image of 9B shows a smaller electrode that is also available for ablations, but is less commonly used.

During the operation, near real-time magnetic resonance thermal imaging (MRTI) is produced, as well as the estimation of the ablation zone, calculated using the correlated temperature values which are then displayed as color-coded images (also referred to as "thermal" images). The technology also estimates cellular death based on temperature history data seen below in figure 10, where doctors can estimate the dosage administered based on the images. Safety standards are set in place by the producers, Visualase, Inc., where the laser is automatically deactivated if the software detects exceeded temperatures and time [49].
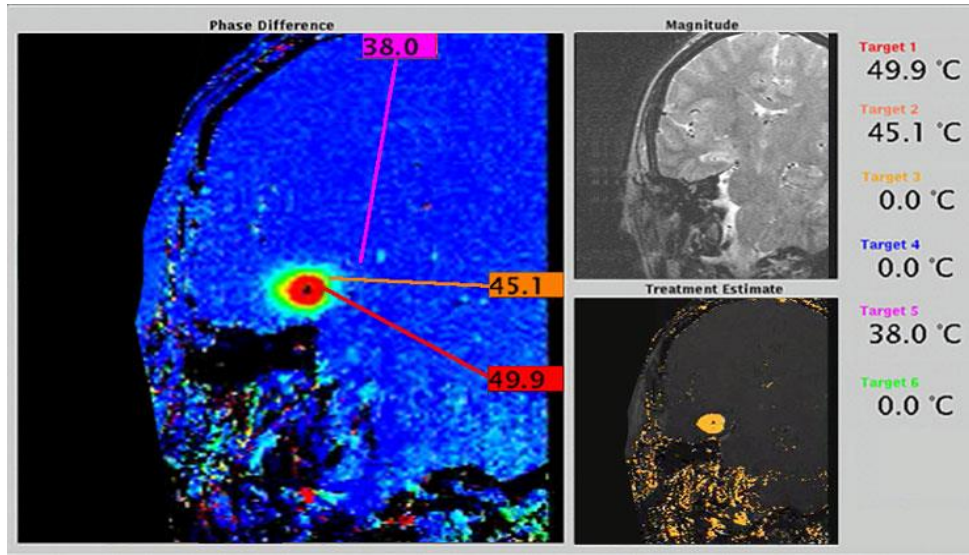
Figure 10. Thermal image of the target area during a laser ablation procedure, with the temperature of the treatments listed vertically on the right [50].

The patients require the use of general anesthesia. During surgery, an MR-compatible Leksell coordinate frame system is used along with CT scanning for placement of the probe, as seen below in figure 11.

Figure 11. Robotic-Guided Stereotactic EEG (ROSA) arm being fitted into a Leksell frame while the patient is inside a CT scanner for real-time imaging of the accuracy of probe placement [51].

Volumetric images are acquired, and the patient is sent to the MRI scanner. At the workstation, the patient's anatomy is visible and co-registration of the image volumes create a reference guide using the MRI scanner and the Leksell frame mentioned earlier. This allows for the visualization of the entry points,

as well as the target area, in 3D view. The trajectory is planned in an X, Y, and Z system using the Leksell frame. A small burr hole, 3-4 mm in diameter, is created through the skull, after fitting, anchoring, and threading the laser applicator, it is inserted to the target area using the robotic-guided stereotactic EEG arm and the Leksell frame. The patient is then taken back to the MRI bed, the applicator is prepared for use, and the MRTI is accomplished before the procedure has begun, and is continuously run during treatment. The laser therapy is performed, as described earlier. The surgeon sets the temperature limits to safely ablate the area and adjust accordingly until all of the desired area is ablated, and treatment is stopped manually by the surgeon. Once the surgeon is satisfied with the ablation at the appropriate targets, a post-procedure fluid attenuated inversion recovery (FLAIR) and T1-weighted contrast series are acquired [40, 49], as seen in figure 12.
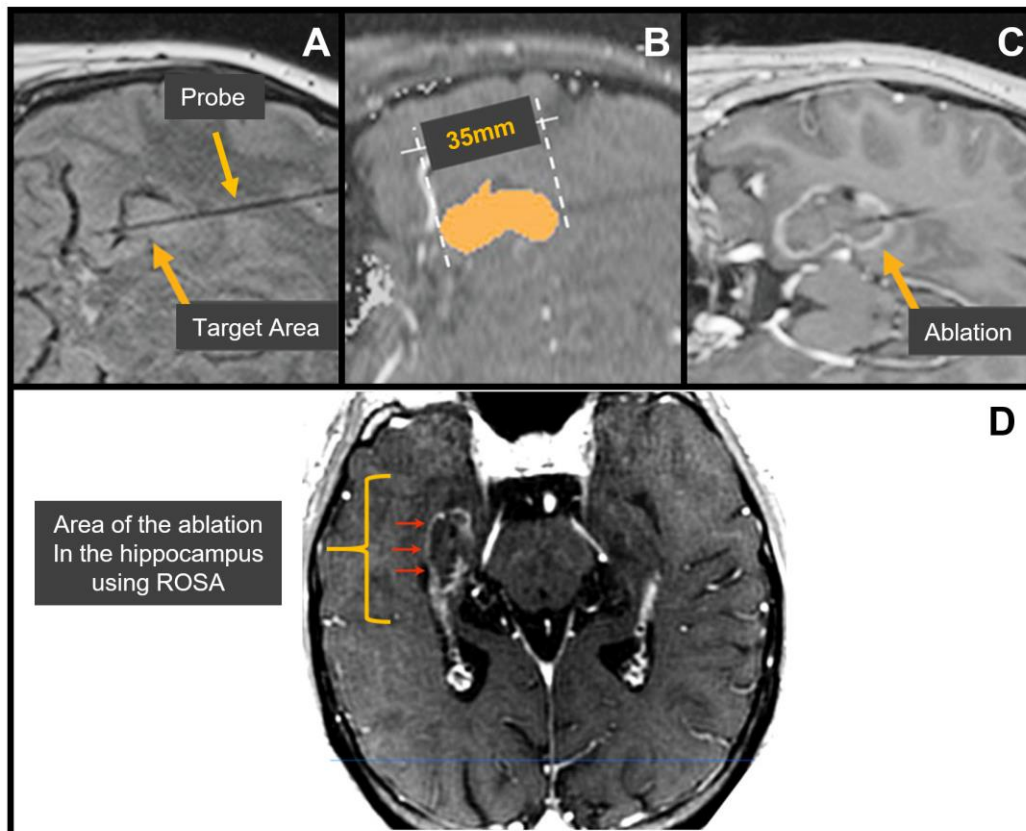
Figure 12. A) Probe insertion and estimation of the target region of the hippocampus [46], B) measurement of the irreversible Damage Zone (orange) during the ablation [46], C) ablated zone in a contrast enhanced T1 image [46], and D) Robotic-guided stereotactic EEG laser ablation of the hippocampus, as seen in a post-operative MRI [42].

The images will confirm this, similar to what is seen in figure 12C and 12D, and the patient is moved away from the magnet, the frame is removed, and a single stitch is used to close the areas of entry. The patient is then observed and discharged within a day. Antibiotics are prescribed for the short term and AEDs are prescribed, as determined by the epileptologist. Follow up evaluations are then performed as established by the patient's doctors in order to determine proper healing and results of the surgery over time, and post-surgery questionnaires about recovery and quality of life are also completed during visits [40].

As mentioned earlier regarding the positives in using a laser ablation method to, in an oversimplified way of stating it, cuts the nerves in question, ablation allows for quicker recovery due to small area of tissue that is disturbed in the process, versus the considerably larger area of tissue that would be disturbed in a traditional resection [40]. It has been found that lasers allow for the minimum necessary amount of apoptosis in the area to occur, and it can be seen in figure 13, as the authors found that looking at a number of types of neurosurgery that occur using lasers, it is one of the most minimally invasive, and allows for the most control when used in conjunction with assistive devices like robots [52].
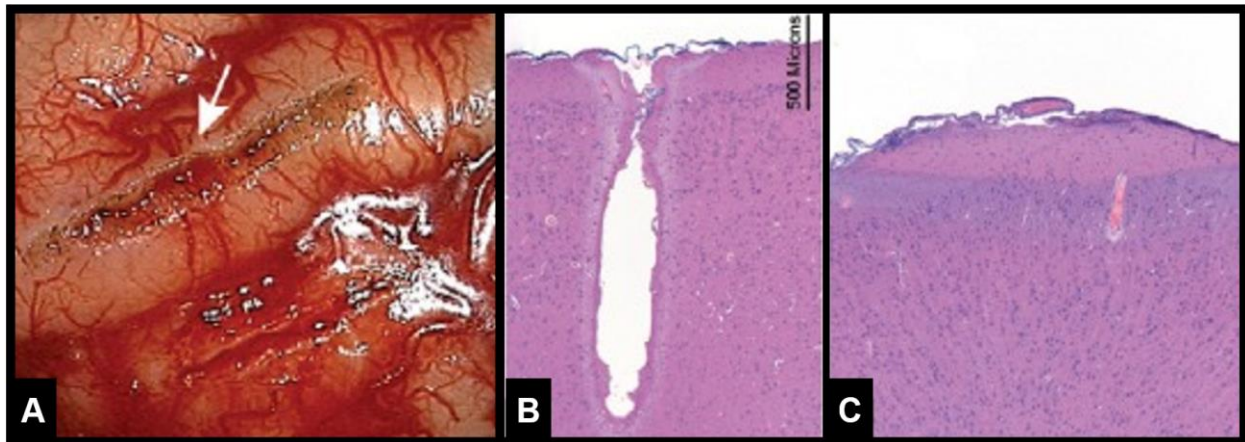
Figure 13. A) A pial incision made using a 7W CO_2 laser, signified by the arrow versus using bipolar micro-scissors, bottom of A, in a porcine brain; B) an H and E stain showing a deep laser cut in brain tissue without extensive damage to the peripheral area; C) small area of visible desiccation and edema, but the pial incision is not visible [52].

Figure 13C, also shows that edema can occur in the usage of lasers, but using them in the controlled, and highly monitored environment, like using the robotic-guided stereotactic EEG system, allows for only the minimal necessary damage to occur, when compared to other surgical methods [52].

1.6 Presurgical Evaluation:

The goals for pre-surgical evaluation can vary, but are usually condensed to five critical points, 1) establishing the correct diagnosis of the epileptic seizure, 2) defining the syndrome electroclinically, 3) delineate any lesions that might be responsible for the seizures, 4) evaluate and select only the most ideal surgical candidates with the most optimal electro-clinico-radiologic correlation, and finally 5) it must be ensured that the surgery will not result in disabling neuropsychological deficits [13]. In pediatric patients, it is vital to observe the number of AEDs/drug resistance to these AEDs, their effectiveness over time, and the need for resection for improvement on the quality of as determined by the epileptologist [13].

1.7 Interictal Spikes and High Frequency Oscillations (HFOs) :

Spikes (1-70Hz) (figure 14 right), which look like sharp waves, are frequently observed in the Seizure Onset Zones [53]. Interictal epileptiform discharges can contain spikes that are present between seizures [8]. Waves and oscillations in the brain are commonly categorized by their frequency or range, often signified by Greek lettering [54, 55]. The kind that is of greatest interest in epilepsy in recent years has been those of higher frequency, above roughly 80Hz, which are commonly referred to as high frequency oscillations, or HFOs [54, 55]. HFOs are classified into ripples (80-250Hz) (figure 14 left) and fast ripples (>250 Hz) and are slightly more difficult to detect using scalp EEGs alone [56, 57]; fast ripples are frequently only seen at low occurrences or not at all in some patients, only being reliably measured in the early stages of epileptogenesis, leading to the conclusion that spikes and ripples are more reliable biomarkers for identification of the Epileptogenic Zone for those with diagnosed medically refractory epilepsy [56, 58].
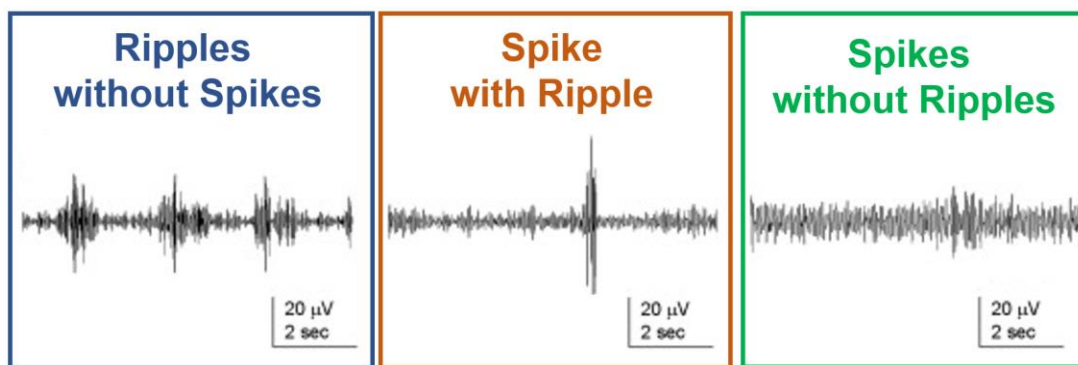
Figure 14. Image example of a ripple without spikes (left, also categorized as an HFO), a ripple co-occurring with a spike (center), and a spike without a ripple (right) over time [modified from 59].

Several studies have shown that fast brain activity recorded with intracranial EEG, specifically HFOs, can be used as biomarkers for epilepsy [54, 56, 60, 61, 62], and used to identify temporal and spatial correlations with the Seizure Onset Zone [63, 64]. Other studies have shown that ripples in HFOs are more accurate than spikes in identifying the Epileptogenic Zone [65, 66]. In 2018, it was discovered that spikes that occur simultaneously with ripples are most closely related to the detection of the Seizure Onset Zone than spikes alone, or the previously mentioned, more promising finding of ripples alone [67], with the event illustrated in the center image of figure 14. Even more so, it has been found in the last decade that surgical resection and lobotomies of the areas where ictal HFOs were detected were correlated with better outcomes post-surgery [65, 68, 69] for those experiencing epilepsy, including for pediatric patients [70] with the main issue being that many times HFOs are also found in physiological areas that do not need to be resected, causing less than ideal surgical outcome. For this reason, there is an urgent need for a biomarker that combines the strengths and weaknesses of identification of areas showing spike and ripple activity, leading to exploration of simultaneous spike and ripple occurrences as that possible biomarker.

1.8 Functional Connectivity

Seizures and interictal epileptic activity are often generated (and spread) in networks which involve one or both hemispheres. Functional connectivity (FC) measures can assess the extent of these networks by quantifying statistical dependencies among remote neurophysiological events. Functional connectivity can be defined in several different ways depending on how it is calculated, but here it will be defined using the classical definition as the study of temporal connections between spatially distinct neurophysiological events [71]. In other words, functional connectivity is defined by statistical relationships when comparing physiologic activity between regions of the brain [72]. This is a quantification of the interactions in specific regions of the brain between two or more time series that are chosen [71, 73]. Again, this can be done using a number of statistical and mathematical methods, with one being to compute and compare the Amplitude Envelope Correlation (AEC), the Phase Locking Value (PLV), and the Correlation (CORR) of the connectivity matrix, although there are many more, each with their advantages and disadvantages [20, 73].

Further understanding the FC matrices, we must know that each color pixel represents a value signifying the connectivity between two signals. In figure 15 we have a matrix to the right with NxN channels. As stated, each pixel is a value representing the two channels' connectivity. The black diagonal from the

top left corner to the bottom right corner represents a comparison of a signal to itself, thus we assume these contain zero values. The signals are collected from each intentionally placed point on the grid electrode. Calculating the connectivity in this manner using iEEG data can give insight into a possibility of development and discovery of a biomarker.
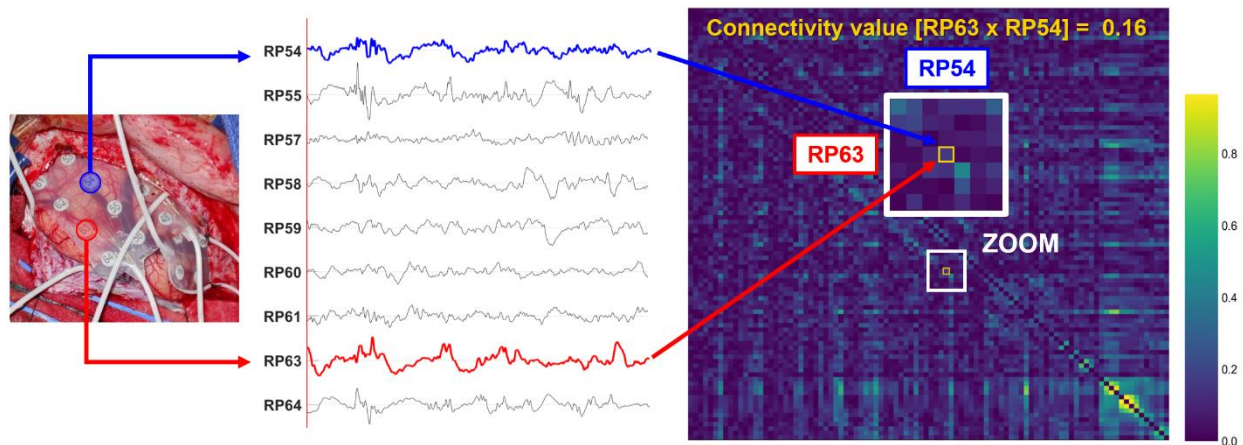
Figure 15. The diagram depicts how functional connectivity is estimated from iEEG. Pairwise functional connectivity matrices (right) are estimated for each patient from iEEG. The blue and green matrix is a connectivity matrix for a brain network comprising of N channels creating an N×N matrix: the diagonal elements of the matrix represent the connectivity of each node with itself. It is assumed that they contain only zero values. Off-diagonal elements of the connectivity matrix represent the connectivity between pairs of distinct channels [74].

To understand functional connectivity in relation to HFO information collected via iEEG, frequencies of 1-250 Hz should be explored that cover the most prominent activity in the human brain. Spikes (1-70 Hz) and ripples (80-250 Hz) are more commonly occurring and frequently seen in many medically refractory epileptic patients [53]. On the other hand, fast ripples (>250 Hz) are very specific biomarkers that are rarely, if at all, seen in patients with refractory epilepsy, with most observable occurrences happening during the early stages of epileptogenesis [56, 58]. IEEGs signals are found in a wide range of frequencies and can be isolated and analyzed for further exploration to determine location of specific activities of interest [75]. These activities of interest, including spikes and ripples, can then be analyzed with the previously mentioned statistical methods in order to identify and define functional connectivity in the Epileptogenic Zone. By looking into simultaneous spike and ripple activity as a biomarker, we fill the gap in the literature currently present for this biomarker, in terms of research into epilepsy, as depicted in figure 16.
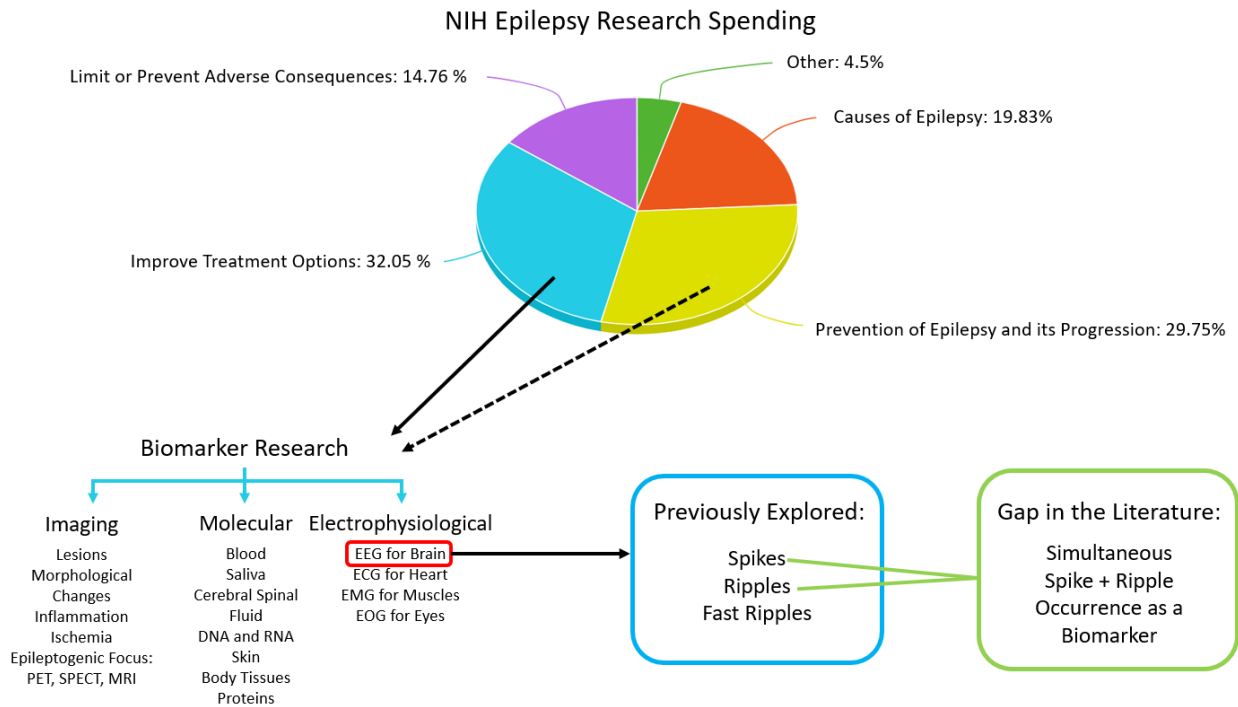
Figure 16. The diagram illustrates National Institute of Health's (NIH) current funding and allocation into different aspects of epilepsy research, and where the novel idea of simultaneous spike and ripple biomarker research stands in this field [76-79].

1.9 Aims of the studies

The main goal of this thesis is to evaluate the efficacy of laser ablation in the neurosurgery of children with refractory epilepsy, and explore the development of a novel interictal functional connectivity biomarker that may identify the Epileptogenic Zone with high precision and potentially improve the surgical outcome of patients undergoing surgery.

To evaluate the efficacy of the robotic-guided stereotactic EEG laser ablation procedure, we retrospectively analyzed the medical records from 36 children with medically refractory epilepsy who have undergone epilepsy surgery with robotic-guided stereotactic EEG laser ablation at Cook Children's Health Care System. We examined the surgical outcome of the patients by their post-surgery Engel scores and the number of AEDs, and conducted t-tests to evaluate differences.

To develop the interictal functional connectivity biomarker of the Epileptogenic Zone, we analyzed iEEG data from 19 patients with medically refractory epilepsy undergone resective surgery (13 with good surgical outcome and 6 with poor surgical outcome). We filtered the iEEG data in the following frequency

bands: 1-70 Hz for spikes, and 80-250 Hz for ripples, and both 1-70 Hz and 80-250 Hz for simultaneous spike and ripple events. Then, we estimated the following functional connectivity matrixes: AEC, PLV, and CORR. We compared these functional connectivity measures for electrodes inside the Seizure Onset Zone and the Resection Zone. We performed statistical analysis between these measures using Wilcoxon signed-rank test.

CHAPTER 2
MATERIALS AND METHODS

2.1 Retrospective Analysis of Medical Records for Robotic-Guided Stereotactic EEG Laser

Ablation Patients Procedures

Using Cook Children's Epilepsy Database containing medical records of patients hospitalized in the epilepsy unit, we identified patients who had undergone the robotic-guided stereotactic EEG laser ablation procedure. We selected patients who satisfied the following inclusion and exclusion criteria: (i) no response to two or more AEDs according to the guidelines of ILAE; (ii) recommendation for laser ablation by a multidisciplinary team consisted of epileptologists, neurologists, neurosurgery, and other health providers; (iii) age during the procedure between 0 and 19 years; (iv) established diagnosis of medically refractory epilepsy between the age of 0 and 19 years of age; and (v) patients undergone laser ablation at Cook Children's Medical Center between 2013 and 2017.

We performed an extensive search and documentation on the identified patients for any information that was found during pre-surgical imaging, official diagnosis of drug resistant epilepsy, semiology and etiology, location and epilepsy localization information, list of current and past AEDs, surgical success, frequency of seizures before and after the procedure, follow up appointment information, information regarding mental wellness and overall physical wellbeing, duration of the stay after the operation/procedure, and any post-operational care. We hypothesized that ILAE Engel outcomes for the laser ablation procedure for both 1-year and 2-year post-procedure would be statistically significant between the years, and that those that were taking 3+ AEDs would have a statistically significant difference when compared to those that were taking 0, 1, or 2 AEDs before surgery, regardless of seizure frequency pre-procedure. To evaluate this, paired and unpaired t-tests were performed.

2.1.1 Statistical Analysis

The data analyses and t-tests were conducted in SPSS and Microsoft Excel.

T-tests were conducted, as it involved comparisons of groups of people. This is a simple statistical calculation normally done when there aren't many factors involved in the calculation, involving only groups

and the sizes of the groups. Alpha for all the tests were set to 0.05. For this reported study, we only conduct paired and unpaired t-tests.

The goal was to identify if the number of AEDs regularly taken directly before the procedure correlated with the outcome of the procedure when compared to those who were taking fewer or greater numbers of AED.

2.2 Analysis of iEEG Data from Children Undergoing Epilepsy Surgery

Using Boston Children's Epilepsy Database containing iEEG, patient history, demographic data of previous patients, and previously consented to research being conducted, a retrospective study was done to analyze functional connectivity using data from Spikes, Ripples, and simultaneous Spikes and Ripple events to possibly better identify the Epileptogenic Zone with higher precision. We selected patients who satisfied the following inclusion and exclusion criteria: (i) no response to 2 or more AEDs, according to the guidelines set by the ILAE and their multidisciplinary care team; (ii) underwent resection, as determined and conducted by their multidisciplinary team consisting of epileptologists, neurologists, neurosurgery, and other health providers; (iii) age during the procedure between 0 and 19 years; (iv) initial seizure onset must have occurred between the ages of infancy to 19 years; (v) patients undergone resection at Boston Children's Hospital between 2011 and 2018.

2.2.1 Functional Connectivity Measures

2.2.1.1 Amplitude Envelope Correlation (AEC)

Amplitude envelope correlation, or AEC, is a way to measure how synchronous identified cortical oscillations are within the individuals. Amplitude envelopes are the Hilbert transformation's absolute value of the identified cortical oscillation. In other words, it reflects energy fluctuations in an oscillation over time. When the energy is high, the amplitude is high. Using the correlated amplitude (energy) envelopes of two oscillatory brain signals, we can calculate the AEC. Synchronous amplitude envelope fluctuations between oscillations or networks can be identified by high AEC values. Functional brain networks can be identified by using these AEC values to identify synchronous patterns, both within and across frequency bands, independent of phase coherence [80, 81]. This allows us to observe functional coupling without phase coherence or coherence.

2.2.1.2 Phase Locking Value (PLV)

Phase Locking Value (PLV) is the most commonly used phase interaction measure; it is "the absolute value of the mean phase difference between the two signals expressed as a complex unit-length vector" [75, 82, 83]. If the marginal distributions for the two signals are the same and each signal is independent of the other, then the relative phase will also have a uniform distribution and the PLV will be zero. Conversely, if the phases of the two signals are strongly coupled then the PLV will approach unity. For event-related studies we would expect the marginal to be uniform across trials unless the phase is locked to a stimulus. As this is an event related study, PLV is a good calculated measure for functional connectivity. In summary, it detects frequency specific transient phase locking, independent from the amplitude that can be found. H. Shahabi *et al.* of Brainstorm (2021) [84] mathematically defined what is used during their calculations as the following:

> Phase synchronization between two narrow-band signals is frequently characterized by the Phase Locking Value (PLV). Consider a pair of real signals $s_1(t)$ and $s_2(t)$, that have been band-pass filtered to a frequency range of interest. Analytic signals can be obtained from $s_1(t)$ and $s_2(t)$ using the Hilbert transform:

$$z_i(t) = s_i(t) + jHT(s_i(t))$$

> Using analytical signals, the relative phase between $z_1(t)$ and $z_2(t)$ can be computed as,

$$\Delta\phi(t) = arg\left(\frac{z_1(t)z_2^*(t)}{|z_1(t)||z_2(t)|}\right)$$

> The instantaneous PLV is

$$PLV(t) = \left|E\left[e^{j\Delta\phi(t)}\right]\right|$$

[84]

2.2.1.3 Correlation Coefficient (CORR)

Correlation is the simplest statistical method to find possible interactions in brain regions. It simply show to the dependence that could be present between two random variable, or in this case EEG signals. It does

have its downfalls, as it cannot explain the association in different frequency bands or reduce the problem of volume conduction, but it can provide a better insight into any associations present between narrow banded signals [20, 71, 73].

The idea of using these three metrics AEC, PLV, and CORR, is that they each measure different aspects of the signals and their interactions, to give us a more rounded view on how these functional connectivity measures can tell us more about the Epileptogenic Zone. Although PLV was previously the most commonly used metric [75, 82, 83], we cannot get a full understanding of the connectivity, since it only measures non-directional frequency specific synchronization [85], as a high PLV would indicate a high synchronization [85, 86, 87]. To make up for this, AEC was included in the assessment, as it is showing great promise in the detection of connectivity in patients with focal epilepsy in recent years [76, 77, 85, 88], and it can also capture different aspects of the connectivity pattern when compared to PLV [88], as mentioned earlier in the AEC and PLV descriptions. CORR was included due to its simple and basic nature of detecting connectivity [20, 71, 73]. With a combination of these three, we can get a fuller view of connectivity, as well as make up for any lacking aspects of measurement.

Figure 17, is an illustration of these average connectivity matrices of all of the individual epochs comparing the values of each signal of the patient.
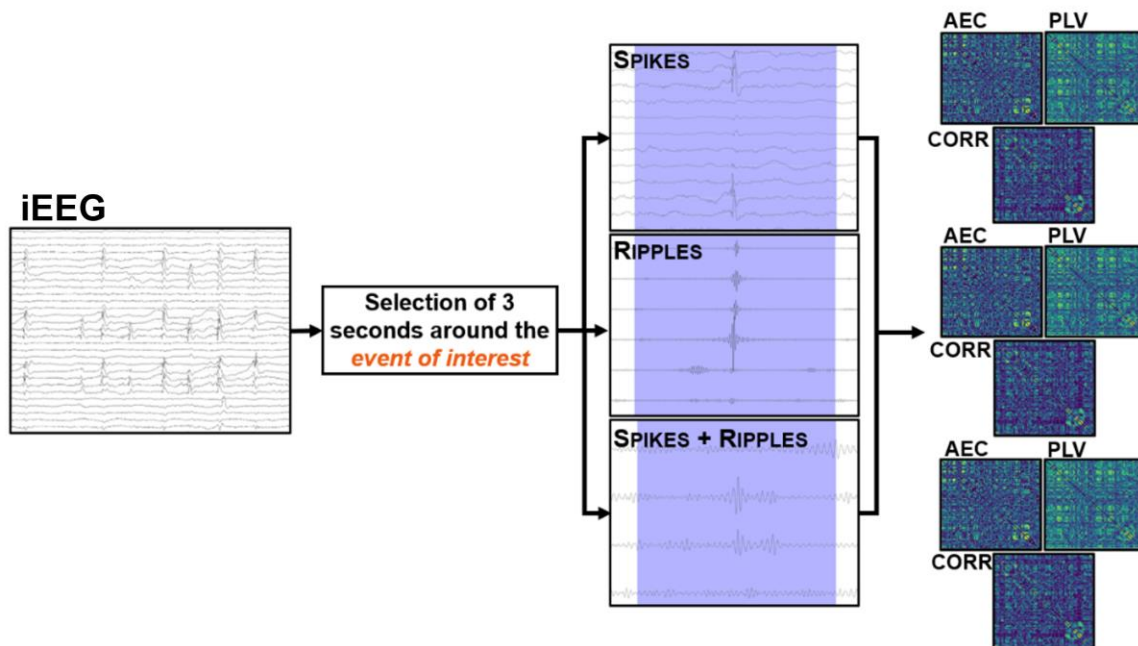
Figure 17. A diagram of the flow of the overall procedures and metrics used for the study, where a single patient's iEEG recording is taken and either spikes, ripples, or simultaneous events of spikes and ripples

were identified in their respective frequencies. From here 1.5 seconds of either side of the event were selected to be evaluated. This was done with all non-overlapping 3 second events. Three separate connectivity matrices, AEC, PLV, and CORR, which contained their respective values between two electrodes, were produced and compared for the inside of the Seizure Onset Zone and the Resection Zone, and the outside of these zones, respectively [inspired by 89].

2.2.2 Procedures for Functional Connectivity Analysis on Data

In this study, functional connectivity analysis was performed by using an open-source software of MATLAB® called *Brainstorm* [90]. was used for data processing for this study. Statistical analyses was conducted in MATLAB®.

Pediatric patients were chosen based on data collected as part of their presurgical evaluation, consisted of noninvasive and invasive (i.e., SEEG and ECOG) monitoring, and who underwent epilepsy surgery. The SEEG and ECOG signal recordings were held in a database, from which they were extracted and uploaded onto *Brainstorm* to be visually analyzed. Using documentation of known artifacts, bad recording times, and bad channels, the channels and epochs of suspicion were examined and then removed. Biological artifacts, such as heart rate and blinking, were also removed.

For each patient, the data were re-referenced and preprocessed in the following way: (i) the DC offset was removed, (ii) the notch filter was applied, as well as standard harmonics (at 60, 120, 180, 240, 300, 360, 420, and 480 Hz) to remove noise, and (iii) the bandpass filters (1-70 Hz) for Spikes, (80-250 Hz) for Ripples, and both (1-70 Hz) and (80-250 Hz) for simultaneous Spikes and Ripples. Two event files consisting of Spikes and Ripples were imported on *Brainstorm* for the analysis of both the Seizure Onset Zone and the Resection Zone, and were also combined to localize the portions that contain both events occurring simultaneously in the signals. We selected epochs of 1.5 seconds before the event, and 1.5 seconds after the event, for a total of 3 seconds.

These epochs were then extracted for functional connectivity analysis. This analysis was done by computing three methods (i.e., AEC, PLV, and CORR) that allow us to generate three matrices containing the functional connectivity values that we compared between inside and outside the regions of interest (Seizure Onset Zone and Resection Zone). For each patient, we obtained an averaged value for each AEC, PLV, and CORR matrix (as illustrated in figure 17) that we used for the statistical analysis (*Wilcoxon signed-rank* test) to observe which measure was significant when comparing the values inside than outside the region, in both good and poor outcome patients, separately for Seizure Onset Zone and Resection Zone.

We hypothesized that increased functional connectivity values would be present inside Seizure Onset Zone and Resection Zone compared to outside. With this hypothesis, we can better understand if this approach based on functional connectivity will help to identify the Epileptogenic Zone, by providing an additional value to the presurgical evaluation of patients with drug resistant epilepsy.

CHAPTER 3

RESULTS

3.1 Robotic-Guided Stereotactic EEG Laser Ablation and Patient Medical History Analysis Results

3.1.1 Demographic Information

Demographic information of the patients chosen and analyzed, based on the criteria set in the Materials and Methods section:

- 36 pediatric epileptic patients did not respond to 2 or more AEDs and were recommended laser ablation by epileptologists, neurologists, and surgeons during a patient conference

- Ages range between 3 years and 19 years old when the procedure was conducted

  o Mean of 11 years of age

- Diagnosed between the ages of infancy (<1 year of age) and 14 years of age

  o Mean of 6 years of age

- 22 males and 14 females

- 35 patients had focal onset epilepsy, 1 had generalized

- Every patient's laser ablation procedures were conducted at Cook Children's Medical Center in Fort Worth, Texas between the years 2013 and 2017

It is important to note that one patient had 3 procedures conducted due to religious restrictions, another patient had 2 ablations after post-procedure evaluations and monitoring determined that another procedure was necessary, unlike 1 procedure that the other patients had. It also must be noted that there were patients that did not return for routine follow-ups post-procedures, as these patients were usually from out of the area and only present with the operating doctor during the procedure. 6 patients did not have initial MRI findings reported. 11 patients had reported previous surgeries. 8 patients had SEEG monitoring done before the laser ablation. Histology was not ordered for any of the 36 patients. Due to these exceptions listed, only ILAE Engel outcomes 1 and 2 years post-procedure and the number of AEDs regularly taken before the procedure were compared, as they were the most completely reported in all of the patients, regardless of follow-up reports and appointments.

Most complete reporting of ILAE Engel outcomes includes 21 patients that were found to have good (Engel score of 1) outcome the first year, 10 that were found to have good outcome the second year. 2 patients did have any information regarding 1 or 2 year outcomes.

3.1.2 1 year versus 2 year ILAE Engel Class Comparison

Table 2. 1-year versus 2-year Engel Classification Comparison

	Daily pre-op seizure frequency	Weekly pre-op seizure frequency	Monthly pre-op seizure frequency
p-value	0.546	0.351	0.182

Paired t-tests comparing 1 year versus 2 year post-operation ILAE Engel outcome classes, categorized by daily, weekly, or monthly seizure frequency pre-op for the laser ablation procedure; α = .05.

3.1.3 T-Test Comparing the Number of AEDs Taken Pre-Operation

Pre-Op Seizure Frequency: Daily

Table 3. 1-year Post-Operation ILAE Engel Classification Comparison

	0 AEDs	1 AEDs	2 AEDs	3+ AEDs
0 AEDs	-	TLD	0.225	0.188
1 AEDs		-	0.225	0.188
2 AEDs			-	0.631
3+ AEDs				-

A comparison of the number of AEDs used before surgery to the 1-year post-surgery ILAE Engel outcome in patients experiencing daily pre-operation seizure frequency; TLD = Too Little Data, α = .05

Table 4. 2-years Post-Operation ILAE Engel Classification Comparison

	0 AEDs	1 AEDs	2 AEDs	3+ AEDs
0 AEDs	-	0.961	0.521	0.745
1 AEDs		-	0.710	0.809
2 AEDs			-	0.852
3+ AEDs				-

A comparison of the number of AEDs used before surgery to the 2-year post-surgery ILAE Engel outcome in patients experiencing daily pre-operation seizure frequency; TLD = Too Little Data, α = .05.

Pre-Operation Seizure Frequency: Weekly

Table 5. 1-year Post-Operation ILAE Engel Classification Comparison

	0 AEDs	1 AEDs	2 AEDs	3+ AEDs
0 AEDs	-	TLD	TLD	TLD
1 AEDs		-	0.080	**0.000574***
2 AEDs			-	0.125
3+ AEDs				-

A comparison of the number of AEDs used before surgery to the 1 year post-surgery ILAE Engel outcome in patients experiencing weekly pre-operation seizure frequency; TLD = Too Little Data, α = .05.

Significance was found in the weekly pre-operational category when comparing the ILAE Engel classifications of those that were taking 1 AEDs to those that were taking 3+ AEDs before surgery.

Table 6. 2-years Post-Operation ILAE Engel Classification Comparison

	0 AEDs	1 AEDs	2 AEDs	3+ AEDs
0 AEDs	-	TLD	TLD	TLD
1 AEDs		-	TLD	TLD
2 AEDs			-	0.173
3+ AEDs				-

A comparison of the number of AEDs used before surgery to the 2-year post-surgery ILAE Engel outcome in patients experiencing weekly pre-operation seizure frequency; TLD = Too Little Data, α = .05.

Pre-Op Seizure Frequency: Monthly

Table 7. 1-year Post-Operation ILAE Engel Classification Comparison

	0 AEDs	1 AEDs	2 AEDs	3+ AEDs
0 AEDs	-	TLD	0.500	TLD
1 AEDs		-	TLD	TLD
2 AEDs			-	TLD
3+ AEDs				-

A comparison of the number of AEDs used before surgery to the 2-year post-surgery ILAE Engel outcome in patients experiencing monthly pre-operation seizure frequency; TLD = Too Little Data, α = .05.

Table 8. 2-years Post-Operation ILAE Engel Classification Comparison

	0 AEDs	1 AEDs	2 AEDs	3+ AEDs
0 AEDs	-	TLD	0.205	TLD
1 AEDs		-	TLD	TLD
2 AEDs			-	TLD
3+ AEDs				-

A comparison of the number of AEDs used before surgery to the 2-year post-surgery ILAE Engel outcome in patients experiencing monthly pre-operation seizure frequency; TLD = Too Little Data, α = .05.

For all of the tables, we observe t-tests of unequal variances, broken down by seizure frequency pre-op, the year that is being looked at, and the number of AEDs reported being taken up to a month before surgery that are being compared for the laser ablation procedure.

3.2 iEEG Data and Functional Connectivity Study Analysis Results

3.2.1 Demographic Information

Demographic information of the patients chosen and analyzed, based on the criteria set in the Materials and Methods section:

- 19 pediatric epileptic patients that did not respond to AEDs and were recommended resection by epileptologists, neurologists, and surgeons during a patient conference
    - 13 good surgical outcome patients
        - Engel score of 1, 1A, or 1B post-surgery; seizure free
    - 6 poor surgical outcome patients
        - Engel score of 2+ post-surgery; not seizure free
- Age at surgery ranged from 2 years to 18 years of age
- Earliest first seizure occurrence beginning at 2 months of age, latest first seizure occurrence beginning at 16 years of age.
    - Mean of 6 years of age
- 11 males and 8 females
- Every patient's procedures were conducted at Boston Children's Hospital in Boston, Massachusetts between the years 2011 and 2018
- Between 72 and 168 electrodes were placed on each patient for observation and measurement
    - Channel types were either ECOG, SEEG, or both

It is important to note that due to inconsistencies in patient history regarding age, the mean for age at surgery was not reported, but does lie within the range.

3.2.2 AEC Graphs of Average Connectivity

Figure 18. AEC of Average Connectivity of inside and outside the Seizure Onset Zone between 1-70 Hz in both good and poor outcome patients.

In the figure above for the comparison of average connectivity for AEC (1-70 Hz), comparing the inside and outside of the Seizure Onset Zone for good and poor outcome patients, significance was not found. The alpha was set to 0.05. The p-values, as well as the average connectivity and standard deviation, are listed in the appendix of this paper, section 5.1.1.
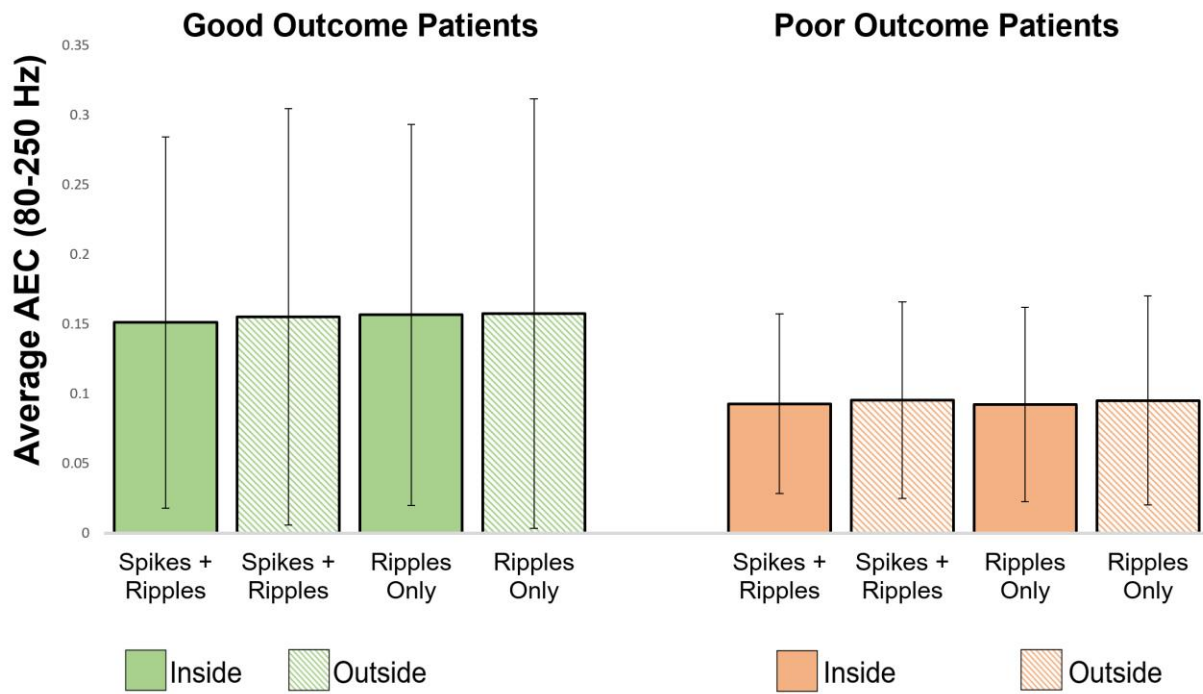
Figure 19. AEC of Average Connectivity of inside and outside the Seizure Onset Zone between 80-250 Hz in both good and poor outcome patients.

In the figure above for the comparison of average connectivity for AEC (80-250 Hz), comparing the inside and outside of the Seizure Onset Zone for good and poor outcome patients, significance was not found. The alpha was set to 0.05. The p-values, as well as the average connectivity and standard deviation, are listed in the appendix of this paper, section 5.1.1.

Figure 20. AEC of Average Connectivity of inside and outside the Resection Zone between 1-70 Hz in both good and poor outcome patients.

In the figure above for the comparison of average connectivity for AEC (1-70 Hz), comparing the inside and outside of the Resection Zone for good and poor outcome patients, significance was not found. The alpha was set to 0.05. The p-values, as well as the average connectivity and standard deviation, are listed in the appendix of this paper, section 5.1.2. The standard deviation bar for Spikes + Ripples on the inside region of the poor outcome patient was too small to visibly display in comparison to the other standard deviation bars.

Figure 21. AEC of Average Connectivity of inside and outside the Resection Zone between 80-250 Hz in both good and poor outcome patients.

In the figure above for the comparison of average connectivity for AEC (80-250 Hz), comparing the inside and outside of the Resection Zone for good and poor outcome patients, significance was not found. The alpha was set to 0.05. The p-values, as well as the average connectivity and standard deviation, are listed in the appendix of this paper, section 5.1.2. The standard deviation bar for Spikes + Ripples on the inside region of the poor outcome patient was too small to visibly display in comparison to the other standard deviation bars.

3.2.3 PLV Graphs of Average Connectivity

Figure 22. PLV of Average Connectivity of inside and outside the Seizure Onset Zone between 1-70 Hz in both good and poor outcome patients.

In the figure above for the comparison of average connectivity for PLV (1-70 Hz), comparing the inside and outside of the Seizure Onset Zone for good and poor outcome patients, significance was not found. The alpha was set to 0.05. The p-values, as well as the average connectivity and standard deviation, are listed in the appendix of this paper, section 5.1.1.
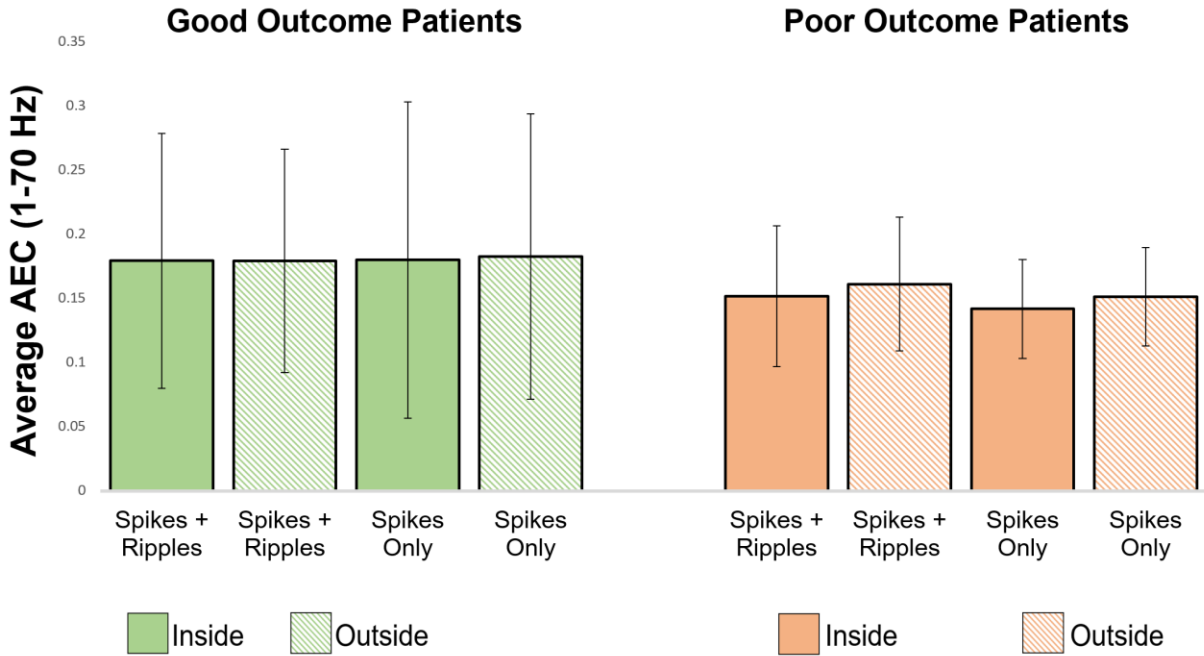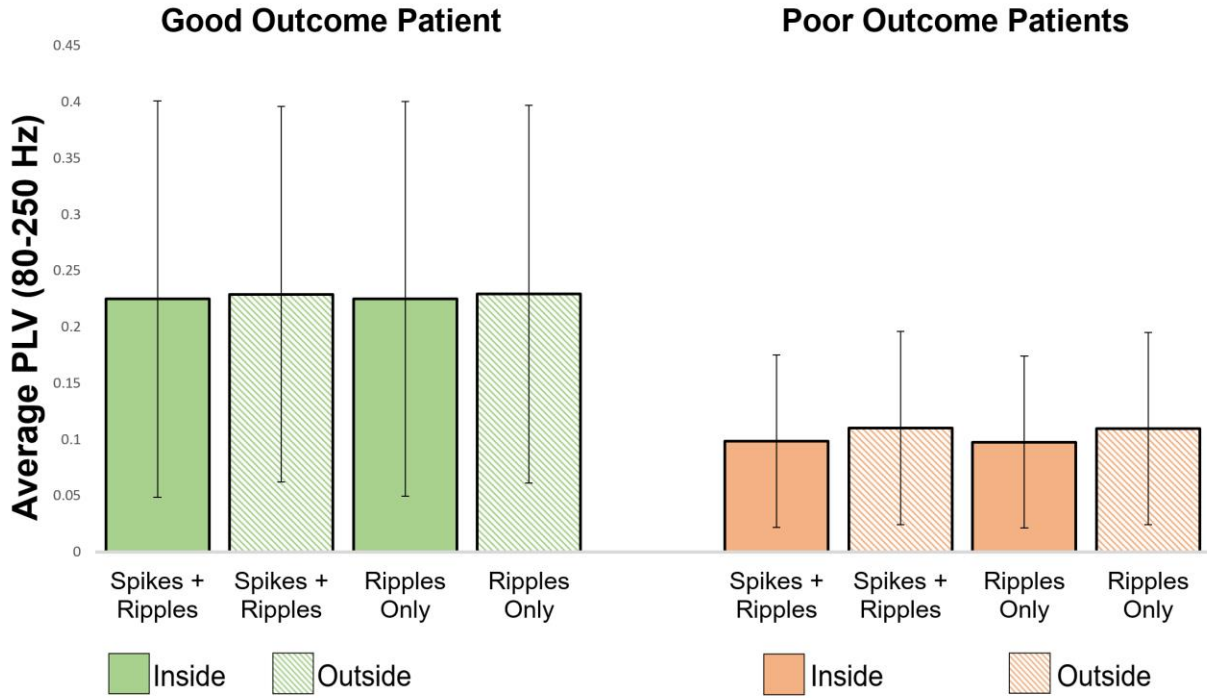
Figure 23. PLV of Average Connectivity of inside and outside the Seizure Onset Zone between 80-250 Hz in both good and poor outcome patients.

In the figure above for the comparison of average connectivity for PLV (80-250 Hz), comparing the inside and outside of the Seizure Onset Zone for good and poor outcome patients, significance was not found. The alpha was set to 0.05. The p-values, as well as the average connectivity and standard deviation, are listed in the appendix of this paper, section 5.1.1.

RESECTION ZONE

Good Outcome Patients **Poor Outcome Patients**

Figure 24. PLV of Average Connectivity of inside and outside the Resection Zone between 1-70 Hz in both good and poor outcome patients.

In the figure above for the comparison of average connectivity for PLV (1-70 Hz), comparing the inside and outside of the Resection Zone for good and poor outcome patients, significance was not found. The alpha was set to 0.05. The p-values, as well as the average connectivity and standard deviation, are listed in the appendix of this paper, section 5.1.2. The standard deviation bar for Spikes + Ripples on the inside region of the poor outcome patient was too small to visibly display in comparison to the other standard deviation bars.

RESECTION ZONE

Figure 25. PLV of Average Connectivity of inside and outside the Resection Zone between 80-250 Hz in both good and poor outcome patients.

In the figure above for the comparison of average connectivity for PLV (80-250 Hz), comparing the inside and outside of the Resection Zone for good and poor outcome patients, significance was not found. The alpha was set to 0.05. The *p*-values, as well as the average connectivity and standard deviation, a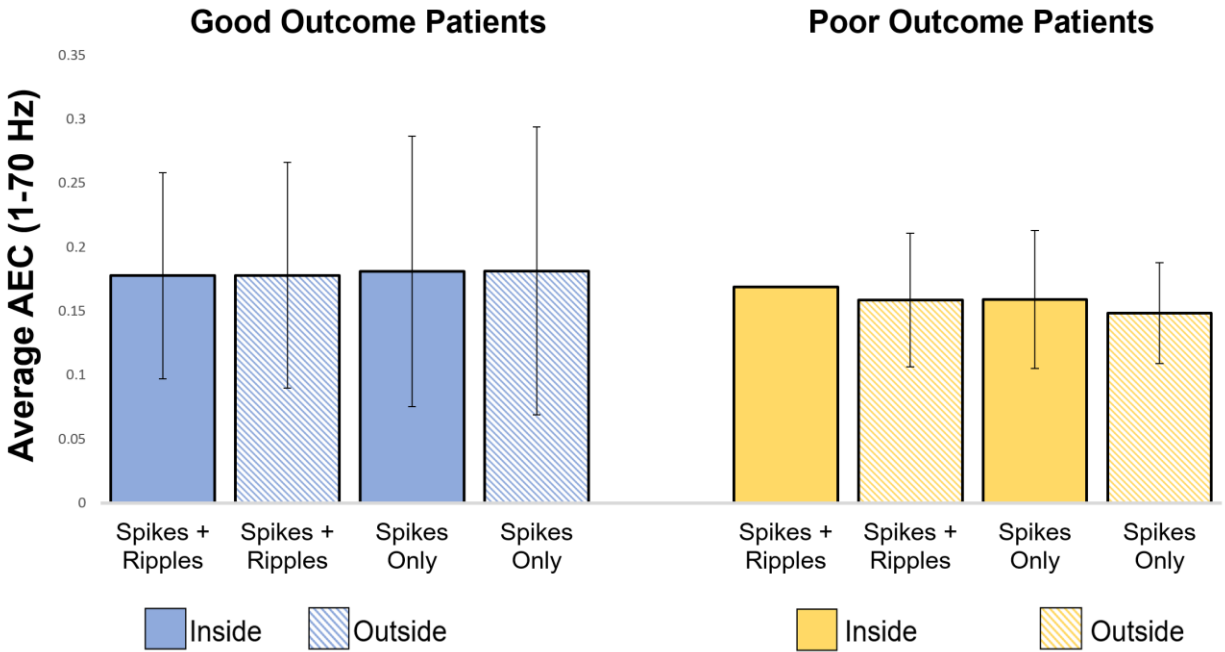re listed in the appendix of this paper, section 5.1.2. The standard deviation bar for Spikes + Ripples on the inside region of the poor outcome patient was too small to visibly display in comparison to the other standard deviation bars.
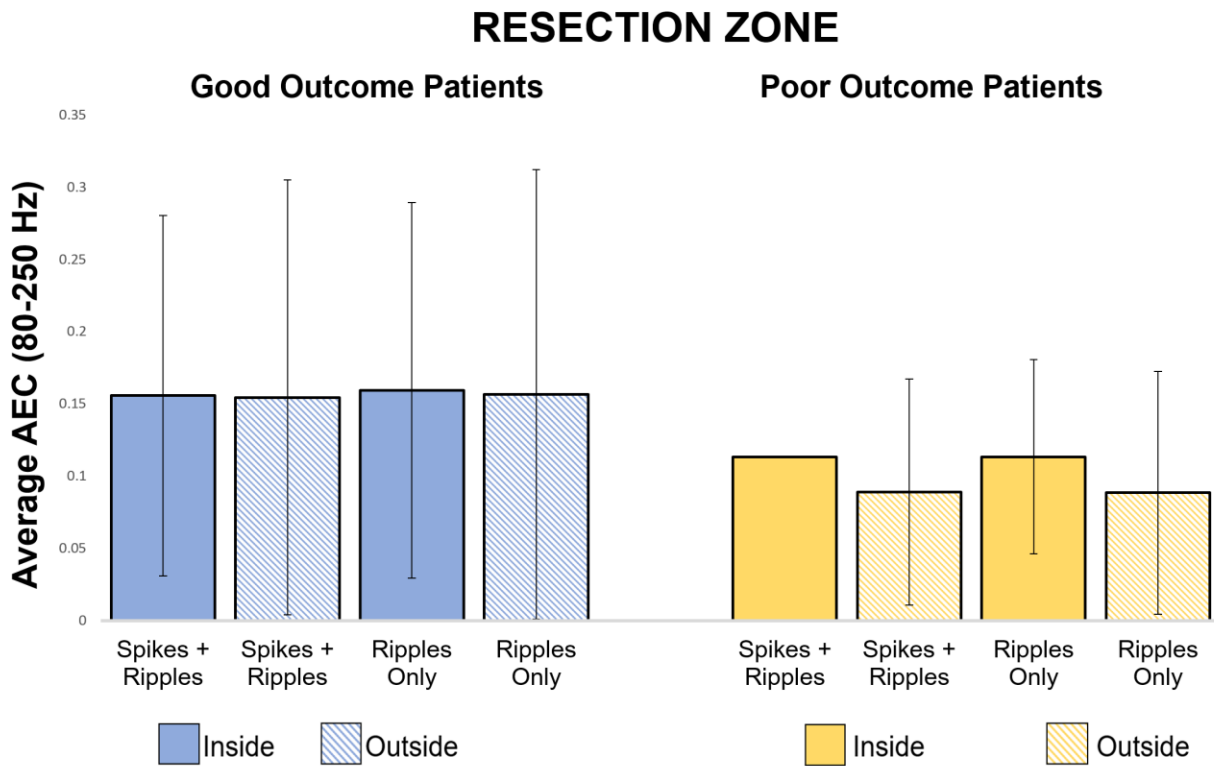
Figure 26. CORR of Average Connectivity of inside and outside the Seizure Onset Zone between 1-70 Hz in both good and poor outcome patients.

In the figure above for the comparison of average connectivity for CORR (1-70 Hz), comparing the inside and outside of the Seizure Onset Zone for good and poor outcome patients, significance was not found. The alpha was set to 0.05. The p-values, as well as the average connectivity and standard deviation, are listed in the appendix of this paper, section 5.1.1.
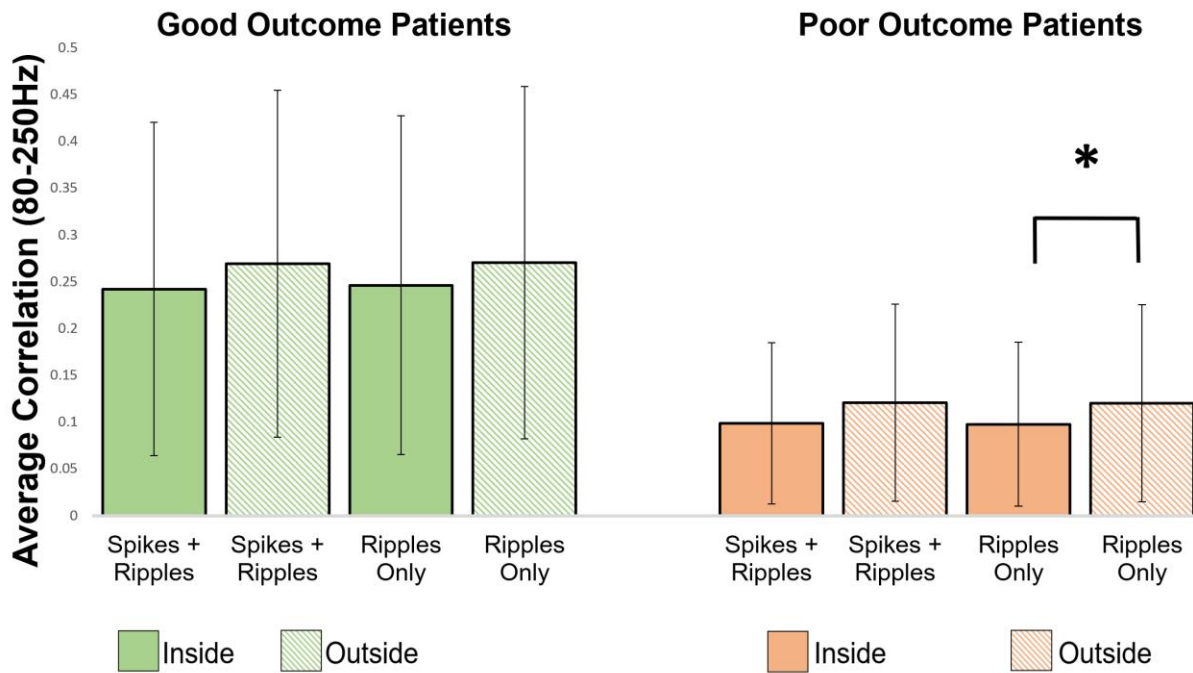
Figure 27. CORR of Average Connectivity of inside and outside the Seizure Onset Zone between 80-250 Hz in both good and poor outcome patients (p = 0.03125; α = .05).

In the figure above for the comparison of average connectivity for CORR (80-250 Hz), comparing the inside and outside of the Seizure Onset Zone for good and poor outcome patients, significance was found when comparing the inside average Seizure Onset Zone connectivity to the outside average Seizure Onset Zone connectivity in poor outcome patients (p = 0.03125; α = .05). The other comparisons were not found to be significant, and alpha was set to 0.05. The p-values, as well as the average connectivity and standard deviation, are listed in the appendix of this paper, section 5.1.1.
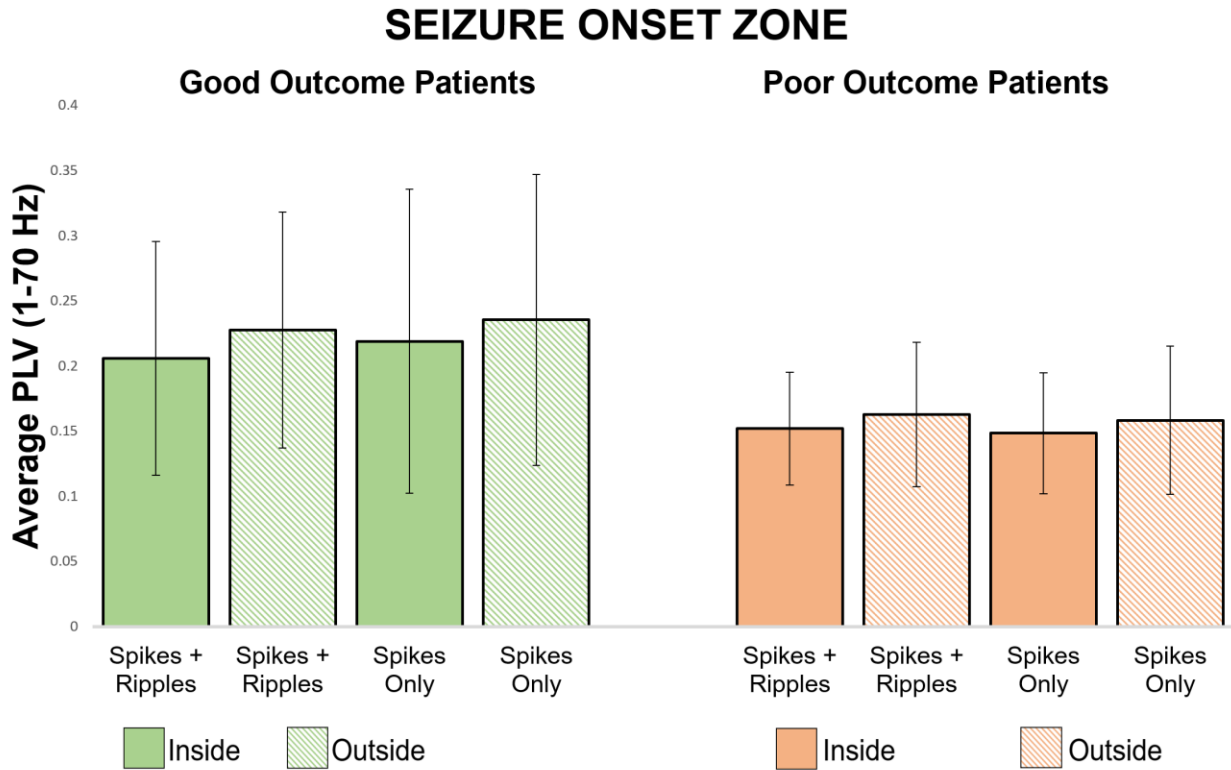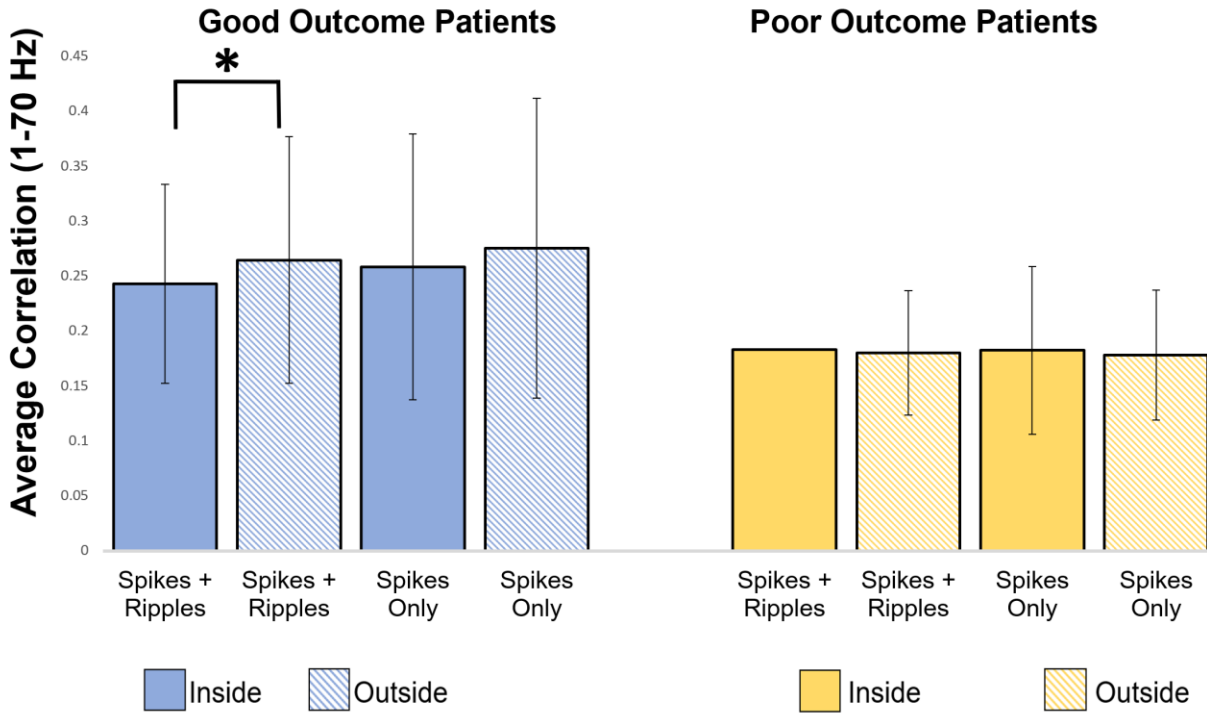
Figure 28. CORR of Average Connectivity of inside and outside the Resection Zone between 1-70 Hz in both good and poor outcome patients (p = 0.03979; α = .05).

In the figure above for the comparison of average connectivity for CORR (1-70 Hz), comparing the inside and outside of the Resection Zone for good and poor outcome patients, significance was found when comparing the inside average Resection Zone connectivity to the outside average Resection Zone connectivity in good outcome patients (p = 0.03979; α = .05). The other comparisons were not found to be significant, and alpha was set to 0.05. The p-values, as well as the average connectivity and standard deviation, are listed in the appendix of this paper, section 5.1.2. The standard deviation bar for Spikes + Ripples on the inside region of the poor outcome patient was too small to visibly display in comparison to the other standard deviation bars.
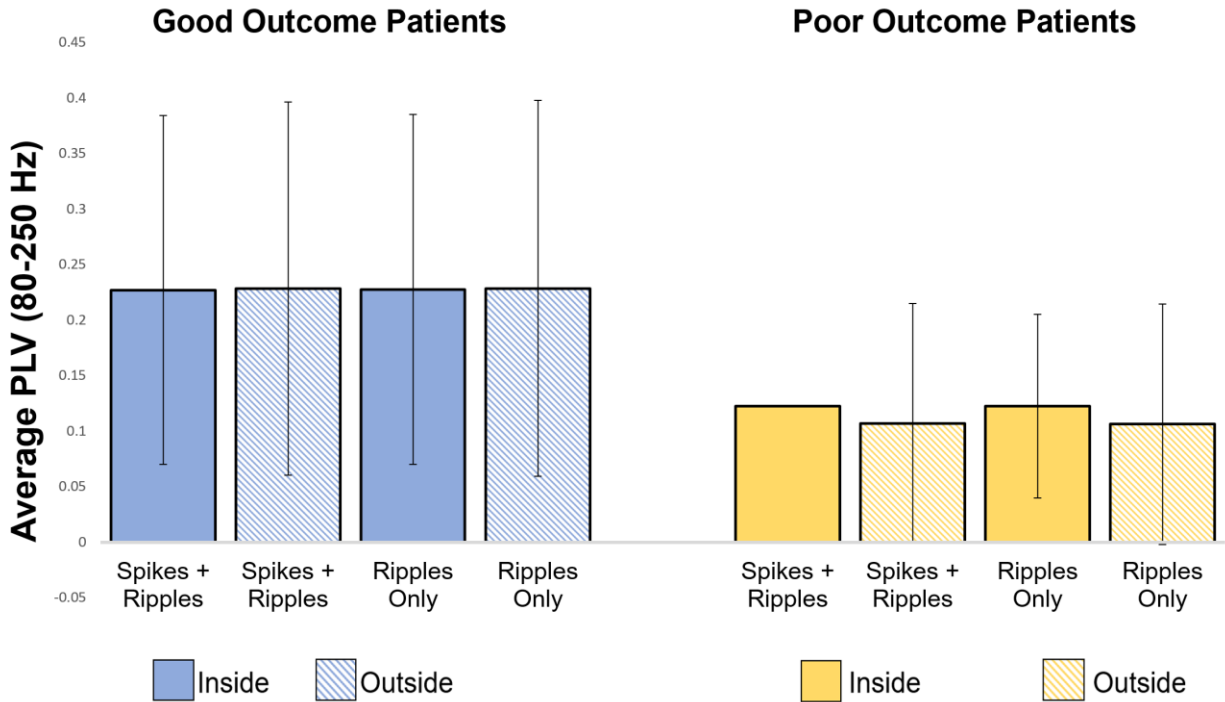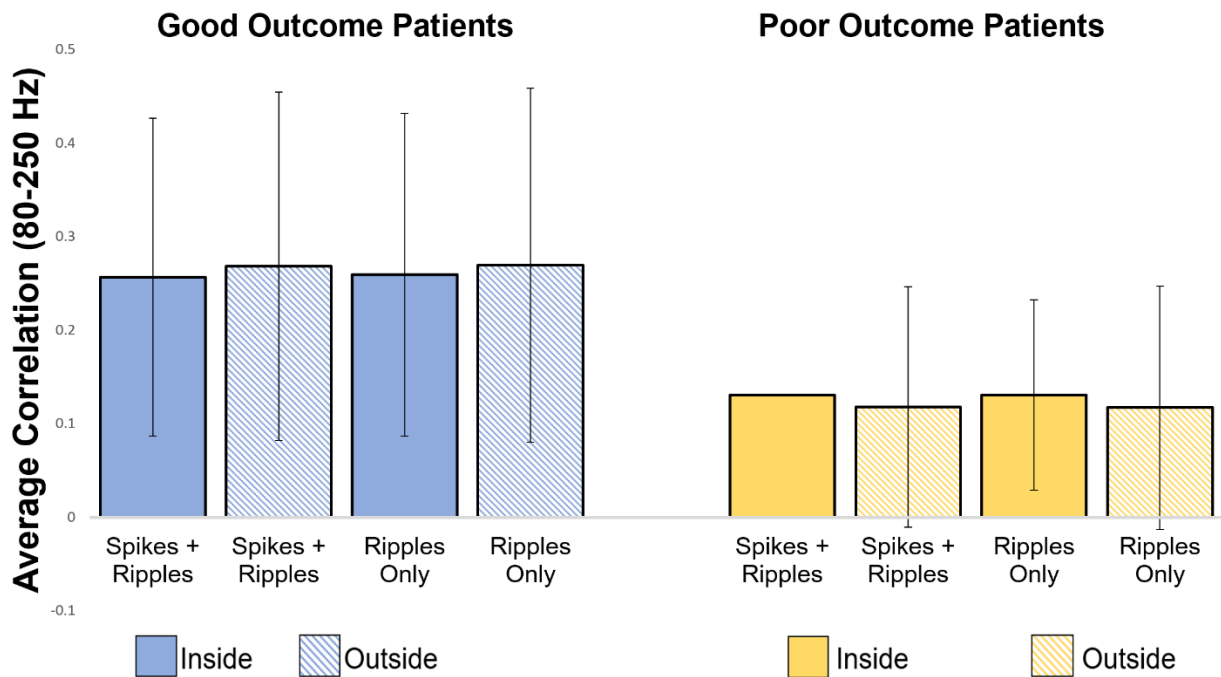
RESECTION ZONE

Figure 29. CORR of Average Connectivity of inside and outside the Resection Zone between 80-250 Hz in both good and poor outcome patients.

In the figure above for the comparison of average connectivity for CORR (80-250 Hz), comparing the inside and outside of the Resection Zone for good and poor outcome patients, significance was not found. The alpha was set to 0.05. The p-values, as well as the average connectivity and standard deviation, are listed in the appendix of this paper, section 5.1.2. The standard deviation bar for Spikes + Ripples on the inside region of the poor outcome patient was too small to visibly display in comparison to the other standard deviation bars.

CHAPTER 4

DISCUSSIONS AND CONCLUSIONS

### 4.1 Robotic-Guided Stereotactic EEG Laser Ablation and Patient Medical History Discussions

When comparing the ILAE post-procedure Engel outcomes of those that were taking 3+ AEDs and experiencing weekly seizures, to the ILAE Engel outcomes of those that were taking 1 AED, a significant difference was found (p-value = 0.000574, α = 0.05), as seen in table 5. The small number of patients that had complete data is likely the cause of the lack of significance in our selected variables, due to the patients not returning for follow ups or opting out of certain pre-surgical neuropsychology evaluations, which can be seen by the number of tests that we could not run because of this issue, signified by TLD in the tables. For this reason, from the analyses of this study, we reject out hypothesis, as all but one test (table 5) was not found to be statistically significant.

Currently, there are not many papers published on pre-procedure AEDs and post-procedure ILAE Engel outcomes on those that have experienced medically refractory epilepsy and have undergone robotic-guided stereotactic EEG laser ablation, besides case studies [91] where researchers suggested that laser ablations could possibly alter the way the blood-brain barrier works possibly causing higher dosages of AEDs to be required in those that continue to require them post-procedure. The case study did not mention pre-procedure AED usage. Another study [92] explored pre-procedural usage of drugs before laser ablation, but tumors were the point of interest, as opposed to causes of epilepsy. As mentioned earlier, this was the reason why AEDs were a point of interest for this present study. The lack of published information is likely due to the same challenges that we faced with the size of our cohort.

Although it was not achieved, the goal of this study was to see if pre- and post-procedural information could give more insight into the efficacy of robotic-guided stereotactic EEG laser ablation for those experiencing medically refractory epilepsy. Even though the other collected variables could not be used, it allows for the potential to further analyze the variables if more patient data is collected and added in the future regarding the outcomes and factors of the patients that have undergone the robotic-guided stereotactic EEG laser ablation procedure. This includes information involving different AEDs that were administered both before and after the procedure, Epileptogenic Zone versus the site of ablation, as well as documentation like post-operational doctor recommendations. Current studies continue to suggest that

the benefits of laser ablation for the treatment of medically refractory epilepsy greatly outweigh the costs [93, 94, 95] due to discomforts, recovery time, and morbidity being greatly reduced compared to traditional resections.

The areas of most interest for future work with this data would be understanding the relationship between doctor recommendations post-operation, types and categories of AEDs prescribed, IQ and behavioral changes before and after the procedure, and changes in medication before and after the procedure. By further understanding and analyzing the factors of the disease, the conclusions made by medical professionals from pre-operational imaging, and obtaining more information on treatment and recommendations post-procedure, we can develop ways to better treat, and possibly even improve customizability of treatment for pediatric patients experiencing drug resistant epilepsy. This would have to be an ongoing study, as more patients would be required to conduct analyses. By making the study long-term multi-campus by having multiple hospitals participate, we would reconcile the issue stated earlier of incomplete data.

4.2 iEEG Data and Functional Connectivity Discussions

As stated earlier, the Epileptogenic Zone is the area of cortex that is necessary for the epileptic seizures to generate. The Seizure Onset Zone is also an area in the cortex where the epileptiform discharges are generated when localized by a scalp or iEEG. In this paper, we analyzed known biomarkers (spikes, ripples, and simultaneous spikes and ripples) from iEEG data, and used metrics such as AEC, PLV, and CORR in order to identify functional connectivity on the inside and outside regions of the Seizure Onset Zone and the Resection Zone. Our hypothesis was that increased functional connectivity values would be present inside Seizure Onset Zone and Resection Zone compared to outside these regions.

We observed a significant difference that was present was when we compared the inside region to the outside region of the Resection Zone in good outcome patients using CORR (1-70 Hz) (figure 28) when observing simultaneous spikes and ripples, which are regarded as more epileptogenic. The $\alpha = 0.05$ and the p-value = 0.03979. This finding tells us that the correlation found in spikes and ripples occurring simultaneously may yield predictive information about the surgical outcome of the patients. With more research, simultaneous occurrences of spikes and ripples may be a reliable biomarker for identification of the Epileptogenic Zone.

We also observed a significant result when comparing the inside and the outside regions of the Seizure Onset Zone in poor outcome patients using CORR (80-250Hz) (figure 27) when observing the ripples only. The $\alpha = 0.05$ and the p-value = 0.03125. The significance found in figure 27 tells us that higher average connectivity was found outside of the determined Seizure Onset Zone than the inside in poor outcome patients.

When we look closer at the insignificant results, we can see that the averages for the insides of both the Seizure Onset Zone and the Resection Zone are lower than the outside (seen in table 9-12 in the appendix). We see this general pattern with the averages occurring with all of the comparisons. Functional connectivity has been found to be higher on the inside of these regions as opposed to outside of these regions [96, 97, 98, 99]. For this reason, we reject our hypothesis for the other tests. This result could be due the methodology of the approach, or that we would have seen a different result if we had a higher number of patients in the cohort, as two similar ongoing studies in the lab where this study was conducted, have found the opposite result when using AEC, PLV, and CORR with spikes, ripples, and simultaneous spikes and ripples for detecting functional connectivity. A review of the methods may lead to a more successful result. The significant result found figure 28 leads us to conclude that there is likely more information that can be gathered when looking at simultaneous occurrences of spikes and ripples as a biomarker for the Epileptogenic Zone.

Seizures are caused by an imbalance of the excitatory and inhibitory neurotransmitters in the brain, which can cause high amounts of electrical activity, which we often see in EEG data [100]. Glutamate, which is an excitatory neurotransmitter, and GABA, which is an inhibitory neurotransmitter, passes between synapses of neurons, allowing for neurons to communicate with each other [100, 101, 102]. Glutamate communicates to the neuron to fire a signal down the line of neurons, while GABA blocks any other neurotransmitters from attaching, stopping the signal flow. Everyone has these neurotransmitters, and they are always flowing no matter what action or emotion is being completed and are usually at a balance in the brain [101, 102]. Excitatory neurons tend to have a refractory period, keeping them from firing for long periods of time [101, 102]. During a seizure, there is an imbalance where the excitatory neurons become overactive and continue firing, causing many neurons to send signals at the same time. This wave-like reaction begins at the Seizure Onset Zone and can go across the brain, interrupting normal activity, causing

the physical symptoms of a seizure [102, 103]. This process is called ictogenesis [103]. Although we know this, we do not fully understand the pathophysiology of epilepsy [100]. We do know that it is a neurological and systemic disorder. The finding in figure 28 regarding using simultaneous spike and ripple activity, supports this well known flow of events that there is a difference in average connectivity when comparing the inside and outside regions of the Resection Zone in good outcome patients.

There is currently no standard diagnostic method of isolating and visualizing this region [8]. The goal of this study was to see if functional connectivity measures, like AEC, PLV, and CORR, could allow for better, more accurate identification of the Epileptogenic Zone when comparing the spikes, ripples, and simultaneous spike and ripple events of the inside of either the Seizure Onset Zone or the Resection Zone, to the outside of the zone. As shown by failing to reject the null hypothesis in all, but two tests, this was not achievable using this methodology, but modifications could allow for a better method of doing so. The study did have a potential for success when posed as an idea for exploration, as seen by other previous studies on spikes, ripples, and simultaneous events being promising potential biomarkers [54, 56, 60-70], and realization of this was not possible at this current moment, but will undoubtedly be with a thorough review.

There is a lot of promise in analyzing iEEG data and signals to better understand the intricacies of this disease, i.e., mapping propagation of spikes, ripples, and fast ripples [104], and localizing these propagations [105]. At the current moment, there is even research being done in virtual, non-invasive techniques to help with pre-surgical evaluation to define the Epileptogenic Zone [74]. Continuing neuroscience research in these directions to better delineate the Epileptogenic Zone would be very beneficial in the advancement of diagnosis and treatment of this childhood illness to help patients gain a higher quality of life.

CHAPTER 5
APPENDIX

5.1 iEEG Functional Connectivity p-values and Average Connectivity

5.1.1 Seizure Onset Zone

Table 9. Good Surgical Outcome Values for the Seizure Onset Zone

Good Surgical Outcome (n=13)			
Comparison	P-values	Average Connectivity Value Inside	Average Connectivity Value Outside
(1-70 Hz) AEC S+R - Inside VS Outside	0.6355	0.1778 ± 0.0805	0.1782 ± 0.0883
(1-70 Hz) PLV S+R - Inside VS Outside	0.2439	0.2166 ± 0.0740	0.2278 ± 0.0929
(1-70 Hz) Corr S+R - Inside VS Outside	**0.03979***	0.2429 ± 0.0904	0.2645 ± 0.1123
(80-250 Hz) AEC S+R - Inside VS Outside	0.3757	0.1557 ± 0.1247	0.1546 ± 0.1506
(80-250 Hz) PLV S+R - Inside VS Outside	0.5417	0.2272 ± 0.1572	0.2285 ± 0.1680
(80-250 Hz) Corr S+R - Inside VS Outside	0.6355	0.2570 ± 0.1701	0.2686 ± 0.1864
(1-70 Hz) AEC OS - Inside VS Outside	0.5417	0.1811 ± 0.1055	0.1816 ± 0.1124
(1-70 Hz) PLV OS - Inside VS Outside	0.4143	0.2268 ± 0.0996	0.2353 ± 0.1137
(1-70 Hz) Corr OS - Inside VS Outside	0.0681	0.2584 ± 0.1208	0.2751 ± 0.1364
(80-250 Hz) AEC OR - Inside VS Outside	0.3054	0.1598 ± 0.1302	0.1568 ± 0.1556
(80-250 Hz) PLV OR - Inside VS Outside	0.5879	0.2276 ± 0.1576	0.2286 ± 0.1693
(80-250 Hz) Corr OR - Inside VS Outside	0.6355	0.2593 ± 0.1726	0.2697 ± 0.1893

P-values were evaluated for the average connectivity value comparison of the inside and outside of the Seizure Onset Zone in the following frequencies, statistical analyses, and for spike, ripples, or simultaneous spikes and ripples for both good ILAE Engel outcome patients. OS = Only Spikes, OR = Only Ripples, and S+R = Spikes and Ripples. α = .05 and significant p-values are signified with a *. The average connectivity value is the average ± standard deviation.

Table 10. Poor Surgical Outcome Values for the Seizure Onset Zone

Poor Surgical Outcome (n=6)			
Comparison	P-values	Average Connectivity Value Inside	Average Connectivity Value Outside
(1-70 Hz) AEC S+R - Inside VS Outside	0.4375	0.1692 ± 0.0521	0.1588 ± 0.0537
(1-70 Hz) PLV S+R - Inside VS Outside	0.4375	0.1641 ± 0.0461	0.1612 ± 0.0577
(1-70 Hz) Corr S+R - Inside VS Outside	0.4375	0.1829 ± 0.0566	0.1802 ± 0.0763
(80-250 Hz) AEC S+R - Inside VS Outside	0.0625	0.1134 ± 0.0783	0.0889 ± 0.0672
(80-250 Hz) PLV S+R - Inside VS Outside	0.3125	0.1228 ± 0.1080	0.1069 ± 0.0828
(80-250 Hz) Corr S+R - Inside VS Outside	0.8438	0.1309 ± 0.1285	0.1179 ± 0.1017
(1-70 Hz) AEC OS - Inside VS Outside	0.4375	0.1592 ± 0.0393	0.1487 ± 0.0403
(1-70 Hz) PLV OS - Inside VS Outside	0.4375	0.1606 ± 0.0488	0.1567 ± 0.0591
(1-70 Hz) Corr OS - Inside VS Outside	0.4375	0.1823 ± 0.0593	0.1781 ± 0.0770
(80-250 Hz) AEC OR - Inside VS Outside	0.0625	0.1134 ± 0.0840	0.0885 ± 0.0711
(80-250 Hz) PLV OR - Inside VS Outside	0.3125	0.1227 ± 0.1083	0.1065 ± 0.0821
(80-250 Hz) Corr OR - Inside VS Outside	0.8438	0.1309 ± 0.1303	0.1171 ± 0.1016

P-values were evaluated for the average connectivity value comparison of the inside and outside of the Seizure Onset Zone in the following frequencies, statistical analyses, and for spike, ripples, or simultaneous spikes and ripples for poor ILAE Engel outcome patients. OS = Only Spikes, OR = Only Ripples, and S+R = Spikes and Ripples. A = .05, and no significance was found in the p-values. The average connectivity value is the average ± standard deviation.

5.1.2 Resection Zone

Table 11.

Table 11. Good Surgical Outcome Values for the Resection Zone

Good Surgical Outcome (n=13)			
Comparison	P-values	Average Connectivity Value Inside	Average Connectivity Value Outside
(1-70 Hz) AEC S+R - Inside VS Outside	0.7869	0.1793 ± 0.0993	0.1791 ± 0.0871
(1-70 Hz) PLV S+R - Inside VS Outside	0.3054	0.2059 ± 0.0897	0.2277 ± 0.0905
(1-70 Hz) Corr S+R - Inside VS Outside	0.2163	0.2252 ± 0.0978	0.2636 ± 0.1097
(80-250 Hz) AEC S+R - Inside VS Outside	1	0.1512 ± 0.1331	0.1554 ± 0.1493
(80-250 Hz) PLV S+R - Inside VS Outside	0.4973	0.2251 ± 0.1762	0.2293 ± 0.1668
(80-250 Hz) Corr S+R - Inside VS Outside	0.2163	0.2423 ± 0.1782	0.2693 ± 0.1855
(1-70 Hz) AEC OS - Inside VS Outside	1	0.1799 ± 0.1233	0.1825 ± 0.1113
(1-70 Hz) PLV OS - Inside VS Outside	0.3396	0.2192 ± 0.1165	0.2355 ± 0.1118
(1-70 Hz) Corr OS - Inside VS Outside	0.2439	0.2471 ± 0.1302	0.2748 ± 0.1344
(80-250 Hz) AEC OR - Inside VS Outside	0.8394	0.1567 ± 0.1367	0.1576 ± 0.1542
(80-250 Hz) PLV OR - Inside VS Outside	0.4973	0.2255 ± 0.1752	0.2293 ± 0.1679
(80-250 Hz) Corr OR - Inside VS Outside	0.2163	0.2464 ± 0.1809	0.2704 ± 0.1882

P-values were evaluated for the average connectivity value comparison of the inside and outside of the Resection Zone in the following frequencies, statistical analyses, and for spike, ripples, or simultaneous spikes and ripples for good ILAE Engel outcome patients. OS = Only Spikes, OR = Only Ripples, and S+R = Spikes and Ripples. α = .05, and no significance was found in the p-values. The average connectivity value is the average ± standard deviation.

Table 12. Poor Surgical Outcome Values for the Resection Zone

Poor Surgical Outcome (n=6)			
Comparison	P-values	Average Connectivity Value Inside	Average Connectivity Value Outside
(1-70 Hz) AEC S+R - Inside VS Outside	1	0.1516 ± 0.0550	0.1611 ± 0.0519
(1-70 Hz) PLV S+R - Inside VS Outside	0.5625	0.1521 ± 0.0432	0.1631 ± 0.0554
(1-70 Hz) Corr S+R - Inside VS Outside	0.4375	0.1637 ± 0.0460	0.1820 ± 0.0732
(80-250 Hz) AEC S+R - Inside VS Outside	0.8438	0.0929 ± 0.0645	0.0955 ± 0.0706
(80-250 Hz) PLV S+R - Inside VS Outside	0.2188	0.0988 ± 0.0766	0.1103 ± 0.0860
(80-250 Hz) Corr S+R - Inside VS Outside	0.0625	0.0988 ± 0.0861	0.1209 ± 0.1053
(1-70 Hz) AEC OS - Inside VS Outside	0.5625	0.1417 ± 0.0386	0.1512 ± 0.0385
(1-70 Hz) PLV OS - Inside VS Outside	0.6875	0.1486 ± 0.0464	0.1585 ± 0.0569
(1-70 Hz) Corr OS - Inside VS Outside	0.5625	0.1639 ± 0.0502	0.1797 ± 0.0740
(80-250 Hz) AEC OR - Inside VS Outside	0.8438	0.0924 ± 0.0698	0.0952 ± 0.0749
(80-250 Hz) PLV OR - Inside VS Outside	0.2188	0.0978 ± 0.0764	0.1099 ± 0.0853
(80-250 Hz) Corr OR - Inside VS Outside	0.03125*	0.0978 ± 0.0876	0.1201 ± 0.1054

*P-values were evaluated for the average connectivity value comparison of the inside and outside of the Resection Zone in the following frequencies, statistical analyses, and for spike, ripples, or simultaneous spikes and ripples for poor ILAE Engel outcome patients. OS = Only Spikes, OR = Only Ripples, and S+R = Spikes and Ripples. α = .05 and significant p-values are signified with a *. The average connectivity value is the average ± standard deviation.*

REFERENCES

[1] R. S. Fisher *et al.*, "ILAE Official Report: A practical clinical definition of epilepsy," *Epilepsia*, vol. 55, no. 4, pp. 475–482, Apr. 2014, doi: 10.1111/epi.12550.

[2] A. Jacoby and J. K. Austin, "Social stigma for adults and children with epilepsy," *Epilepsia*, vol. 48, no. s9, pp. 6–9, Nov. 2007, doi: 10.1111/j.1528-1167.2007.01391.x.

[3] M. M. Zack, "National and State Estimates of the Numbers of Adults and Children with Active Epilepsy — United States, 2015," *MMWR. Morbidity and Mortality Weekly Report*, vol. 66, Aug. 2017, doi: 10.15585/mmwr.mm6631a1.

[4] S. A. Russ, K. Larson, and N. Halfon, "A national profile of childhood epilepsy and seizure disorder," *Pediatrics*, vol. 129, no. 2, pp. 256–64, Jan. 2012, doi: 10.1542/peds.2010-1371.

[5] A. Tolaymat, A. Nayak, J. D. Geyer, S. K. Geyer, and P. R. Carney, "Diagnosis and Management of Childhood Epilepsy," *Current Problems in Pediatric and Adolescent Health Care*, vol. 45, no. 1, pp. 3–17, Jan. 2015, doi: 10.1016/j.cppeds.2014.12.002.

[6] C. S. Andrade and C. D. C. Leite, "Malformations of cortical development: current concepts and advanced neuroimaging review," *Arquivos de Neuro-Psiquiatria*, vol. 69, no. 1, pp. 130–138, Feb. 2011, doi: 10.1590/s0004-282x2011000100024.

[7] D. C. Preston, "Magnetic Resonance Imaging (MRI) of the Brain and Spine: Basics," *Case*, Jul. 04, 2016. https://case.edu/med/neurology/NR/MRI%20Basics.htm.

[8] F. Rosenow and H. Lüders, "Presurgical evaluation of epilepsy," *Brain*, vol. 124, no. 9, pp. 1683–1700, Sep. 2001, doi: 10.1093/brain/124.9.1683.

[9] I. Valencia, D. L. Holder, S. L. Helmers, J. R. Madsen, and J. J. Riviello, "Vagus nerve stimulation in pediatric epilepsy: a review," *Pediatric Neurology*, vol. 25, no. 5, pp. 368–376, Nov. 2001, doi: 10.1016/s0887-8994(01)00319-8.

[10] L.-M. Terrier, M. Lévêque, and A. Amelot, "Brain Lobotomy: A Historical and Moral Dilemma with No Alternative?," *World Neurosurgery*, vol. 132, pp. 211–218, Dec. 2019, doi: 10.1016/j.wneu.2019.08.254.

[11] E. Wyllie, Y. G. Comair, P. Kotagal, J. Bulacio, W. Bingaman, and P. Ruggieri, "Seizure outcome after epilepsy surgery in children and adolescents," *Annals of Neurology*, vol. 44, no. 5, pp. 740–748, Nov. 1998, doi: 10.1002/ana.410440507.

[12] J. H. Cross, "Epilepsy Surgery in Childhood," *Epilepsia*, vol. 43, pp. 65–70, Jun. 2002, doi: 10.1046/j.1528-1157.43.s.3.6.x.

[13] S. Jayalakshmi, S. Vooturi, S. Gupta, and M. Panigrahi, "Epilepsy surgery in children," *Neurology India*, vol. 65, no. 3, p. 485, 2017, doi: 10.4103/neuroindia.ni_1033_16.

[14] M. Dennis, B. J. Spiegler, J. J. Juranek, E. D. Bigler, O. C. Snead, and J. M. Fletcher, "Age, Plasticity, and Homeostasis In Childhood Brain Disorders," *Neuroscience and biobehavioral reviews*, vol. 37, no. 10 0 2, Dec. 2013, doi: 10.1016/j.neubiorev.2013.09.010.

[15] M. V. Johnston, A. Ishida, W. N. Ishida, H. B. Matsushita, A. Nishimura, and M. Tsuji, "Plasticity and injury in the developing brain," *Brain and Development*, vol. 31, no. 1, pp. 1–10, Jan. 2009, doi: 10.1016/j.braindev.2008.03.014.

[16] E. Wyllie, B. E. Gidal, H. P. Goodkin, and G. D. Cascino, *Wyllies treatment of epilepsy: principles and practice.* Philadelphia: Wolters Kluwer/Lippincott Williams & Wilkins, 2011.

[17] W. Penfield and H. Steelman, "THE TREATMENT OF FOCAL EPILEPSY BY CORTICAL EXCISION," *Annals of Surgery*, vol. 126, no. 5, pp. 740–762, Nov. 1947, doi: 10.1097/00000658-194711000-00008.

[18] E. Magiorkinis, A. Diamantis, K. Sidiropoulou, and C. Panteliadis, "Highights in the History of Epilepsy: The Last 200 Years," *Epilepsy Research and Treatment*, vol. 2014, pp. 1–13, 2014, doi: 10.1155/2014/582039.

[19] P. Bailey, "THE SURGICAL TREATMENT OF PSYCHOMOTOR EPILEPSY," *Journal of the American Medical Association*, vol. 145, no. 6, p. 365, Feb. 1951, doi: 10.1001/jama.1951.02920240001001.

[20] H. O. Lüders, I. Najm, D. Nair, P. Widdess-Walsh, and W. Bingman, "The Epileptogenic Zone: General Principles."

[21] C. Carlson and O. Devinsky, "The excitable cerebral cortex," *Epilepsy & Behavior*, vol. 15, no. 2, pp. 131–132, Jun. 2009, doi: 10.1016/j.yebeh.2009.03.002.

[22] M. Omrani, M. T. Kaufman, N. G. Hatsopoulos, and P. D. Cheney, "Perspectives on classical controversies about the motor cortex," *Journal of Neurophysiology*, vol. 118, no. 3, pp. 1828–1848, Sep. 2017, doi: 10.1152/jn.00795.2016.

[23] B. P. Delhaye, K. H. Long, and S. J. Bensmaia, "Neural Basis of Touch and Proprioception in Primate Cortex," *Comprehensive Physiology*, vol. 8, no. 4, pp. 1575–1602, Sep. 2018, doi: 10.1002/cphy.c170033.

[24] Y. Nakai, J.-won Jeong, E. C. Brown, R. Rothermel, K. Kojima, T. Kambara, A. Shah, S. Mittal, S. Sood, and E. Asano, "Three- and four-dimensional mapping of speech and language in patients with epilepsy," *Brain*, vol. 140, no. 5, pp. 1351–1370, 2017.

[25] G Buzsáki, *Rhythms of the brain*. Oxford ; New York: Oxford University Press, 2006.

[26] E. R. Kandel and E. Al, *Principles of neural science*, vol. 4. New York ; Toronto: Mcgraw-Hill Medical, 2000, pp. 1227–1246.

[27] G. Buzsáki, C. A. Anastassiou, and C. Koch, "The origin of extracellular fields and currents — EEG, ECoG, LFP and spikes," *Nature Reviews Neuroscience*, vol. 13, no. 6, pp. 407–420, May 2012, doi: 10.1038/nrn3241.

[28] Y. Wang, J. Yan, J. Wen, T. Yu, and X. Li, "An Intracranial Electroencephalography (iEEG) Brain Function Mapping Tool with an Application to Epilepsy Surgery Evaluation," *Frontiers in Neuroinformatics*, vol. 10, Apr. 2016, doi: 10.3389/fninf.2016.00015.

[29] N. E. Crone, A. Sinai, and A. Korzeniewska, "High-frequency Gamma Oscillations and Human Brain Mapping with Electrocorticography," *Progress in Brain Research*, pp. 275–295, 2006, doi: 10.1016/s0079-6123(06)59019-3.

[30] H. H. Jasper and L. Carmichael, "ELECTRICAL POTENTIALS FROM THE INTACT HUMAN BRAIN," *Science*, vol. 81, no. 2089, pp. 51–53, Jan. 1935, doi: 10.1126/science.81.2089.51.

[31] M. S. Berger and G. A. Ojemann, "Intraoperative Brain Mapping Techniques in Neuro-Oncology," *Stereotactic and Functional Neurosurgery*, vol. 58, no. 1–4, pp. 153–161, 1992, doi: 10.1159/000098989.

[32] K. Iida and H. Otsubo, "Stereoelectroencephalography: Indication and Efficacy," *Neurologia medico-chirurgica*, vol. 57, no. 8, pp. 375–385, 2017, doi: 10.2176/nmc.ra.2017-0008.

[33] F. Cardinale *et al.*, "Stereoelectroencephalography," *Neurosurgery*, vol. 72, no. 3, pp. 353–366, Nov. 2013, doi: 10.1227/neu.0b013e31827d1161.

[34] S. Tocchio, B. Kline-Fath, E. Kanal, V. J. Schmithorst, and A. Panigrahy, "MRI Evaluation and Safety in the Developing Brain," *Seminars in perinatology*, vol. 39, no. 2, pp. 73–104, Mar. 2015, doi: 10.1053/j.semperi.2015.01.002.

[35] A. M. Mathur, J. J. Neil, and T. E. Inder, "Understanding Brain Injury and Neurodevelopmental Disabilities in the Preterm Infant: The Evolving Role of Advanced Magnetic Resonance Imaging," *Seminars in Perinatology*, vol. 34, no. 1, pp. 57–66, Feb. 2010, doi: 10.1053/j.semperi.2009.10.006.

[36] O. A. Glenn, "MR imaging of the fetal brain," *Pediatric Radiology*, vol. 40, no. 1, pp. 68–81, Nov. 2010, doi: 10.1007/s00247-009-1459-3.

[37] M. de Curtis and M. Avoli, "Interictal epileptiform discharges in partial epilepsy: Neurobiologic mechanisms based on clinical and experimental evidence," *Epilepsia*, vol. 51, pp. 22–22, Dec. 2010.

[38] K. M. Earle, S. Carpenter, U. Roessmann, M. A. Ross, J. R. Hayes, and E. Zeitler, "Central Nervous System Effects of Laser Radiation," *Federation Procedings*, vol. 24, no. 1, pp. 129–139, Jan. 1965.

[39] S. Fine *et al.*, "Interaction of Laser Radiation with Biologic Systems," *Federal Procedings*, vol. 14, pp. 35–47, Jan. 1965.

[40] Z. Tovar-Spinoza, D. Carter, D. Ferrone, Y. Eksioglu, and S. Huckins, "The use of MRI-guided laser-induced thermal ablation for epilepsy," *Child's Nervous System*, vol. 29, no. 11, pp. 2089–2094, Jun. 2013, doi: 10.1007/s00381-013-2169-6.

[41] Radiology Society of North America and American College of Radiology, "Children's (Pediatric) CT (Computed Tomography)," *Radiologyinfo.org*, Jan. 30, 2019. https://www.radiologyinfo.org/en/info/pedia-ct (accessed Apr. 09, 2021).

[42] University of Pittsburgh Neurosurgery, "ROSA (Robotic Stereotactic Assistance)," *Neurological Surgery*. https://neurosurgery.secure.pitt.edu/centers-excellence/epilepsy-and-movement-disorders-program/rosa (accessed Apr. 05, 2021).

[43] P. T. Sanders, B. J. Cysyk, and M. A. Bare, "Safety in Long-Term EEG/Video Monitoring," *Journal of Neuroscience Nursing*, vol. 28, no. 5, pp. 305–313, Oct. 1996, doi: 10.1097/01376517-199610000-00004.

[44] M. J. LaRiviere and R. E. Gross, "Stereotactic Laser Ablation for Medically Intractable Epilepsy: The Next Generation of Minimally Invasive Epilepsy Surgery," *Frontiers in Surgery*, vol. 3, Dec. 2016, doi: 10.3389/fsurg.2016.00064.

[45] Medtronic, "Visualase® | MRI-Guided Laser Ablation | Medtronic," . https://www.medtronic.com/us-en/healthcare-professionals/products/neurological/laser-ablation/visualase.html (accessed Apr. 05, 2021).

[46] M. J. LaRiviere and R. E. Gross, "Stereotactic Laser Ablation for Medically Intractable Epilepsy: The Next Generation of Minimally Invasive Epilepsy Surgery," *Frontiers in Surgery*, vol. 3, Dec. 2016, doi: 10.3389/fsurg.2016.00064.

[47] A. Carpentier *et al.*, "Real-time Magnetic Resonance-guided Laser Thermal Therapy for Focal Metastatic Brain Tumors," *Operative Neurosurgery*, vol. 63, no. suppl_1, pp. ONS21–ONS29, Jul. 2008, doi: 10.1227/01.neu.0000311254.63848.72.

[48] D. J. Curry, A. Gowda, R. J. McNichols, and A. A. Wilfong, "MR-guided stereotactic laser ablation of epileptogenic foci in children," *Epilepsy & Behavior*, vol. 24, no. 4, pp. 408–414, Aug. 2012, doi: 10.1016/j.yebeh.2012.04.135.

[49] J. D. Poorter, C. D. Wagter, Y. D. Deene, C. Thomsen, F. Ståhlberg, and E. Achten, "Noninvasive MRI Thermometry with the Proton Resonance Frequency (PRF) Method:In Vivo Results in Human Muscle," *Magnetic Resonance in Medicine*, vol. 33, no. 1, pp. 74–81, Jan. 1995, doi: 10.1002/mrm.1910330111.

[50] Minnesota Epilepsy Group, "Laser Ablation for Epilepsy," *MN Epilepsy Group*, Jun. 05, 2014. https://mnepilepsy.org/services/laser-ablation-for-epilepsy/ (accessed Apr. 05, 2021).

[51] Medtech SA and Medical Design & Outsourcing, "Robot that assists in brain surgery cuts procedure time in half," *Medical Design and Outsourcing*, Aug. 18, 2015. https://www.medicaldesignandoutsourcing.com/robot-that-assists-in-brain-surgery-cuts-procedure-time-in-half/ (accessed Apr. 05, 2021).

[52] M. Preul *et al.*, "Laser application in neurosurgery," *Surgical Neurology International*, vol. 8, no. 1, p. 274, 2017, doi: 10.4103/sni.sni_489_16.

[53] M. A. Kramer *et al.*, "Scalp recorded spike ripples predict seizure risk in childhood epilepsy better than spikes," *Brain*, vol. 142, no. 5, pp. 1296–1309, Mar. 2019, doi: 10.1093/brain/awz059.

[54] G. Buzsáki and F. L. da Silva, "High frequency oscillations in the intact brain," *Progress in Neurobiology*, vol. 98, no. 3, pp. 241–249, Sep. 2012, doi: 10.1016/j.pneurobio.2012.02.004.

[55] J. Engel Jr, A. Bragin, R. Staba, and I. Mody, "High-frequency oscillations: What is normal and what is not?," *Epilepsia*, vol. 50, no. 4, pp. 598–604, Apr. 2009, doi: 10.1111/j.1528-1167.2008.01917.x.

[56] J. D. Jirsch, E. Urrestarazu, P. LeVan, A. Olivier, F. Dubeau, and J. Gotman, "High-frequency oscillations during human focal seizures," *Brain*, vol. 129, no. 6, pp. 1593–1608, Apr. 2006, doi: 10.1093/brain/awl085.

[57] R. J. Staba, C. L. Wilson, A. Bragin, I. Fried, and J. Engel, "Quantitative Analysis of High-Frequency Oscillations (80–500 Hz) Recorded in Human Epileptic Hippocampus and Entorhinal Cortex," *Journal of Neurophysiology*, vol. 88, no. 4, pp. 1743–1752, Oct. 2002, doi: 10.1152/jn.2002.88.4.1743.

[58] A. Bragin, I. Mody, C. L. Wilson, and J. Engel, "Local Generation of Fast Ripples in Epileptic Brain," *The Journal of Neuroscience*, vol. 22, no. 5, pp. 2012–2021, Mar. 2002, doi: 10.1523/jneurosci.22-05-02012.2002.

[59] V. Sagi and M. S. Evans, "Relationship between high-frequency oscillations and spikes in a case of temporal lobe epilepsy," *Epilepsy & Behavior Case Reports*, vol. 6, pp. 10–12, 2016, doi: 10.1016/j.ebcr.2016.04.006.

[60] J. Jacobs *et al.*, "High-frequency Oscillations (HFOs) in Clinical Epilepsy," *Progress in Neurobiology*, vol. 98, no. 3, pp. 302–315, Sep. 2012, doi: 10.1016/j.pneurobio.2012.03.001.

[61] R. S. Fisher, W. R. S. Webber, R. P. Lesser, S. Arroyo, and S. Uematsu, "High-Frequency EEG Activity at the Start of Seizures," *Journal of Clinical Neurophysiology*, vol. 9, no. 3, pp. 441–448, Jul. 1992, doi: 10.1097/00004691-199207010-00012.

[62] M. Zijlmans, P. Jiruska, R. Zelmann, F. S. S. Leijten, J. G. R. Jefferys, and J. Gotman, "High-frequency oscillations as a new biomarker in epilepsy," *Annals of Neurology*, vol. 71, no. 2, pp. 169–178, Feb. 2012, doi: 10.1002/ana.22548.

[63] G. A. Worrell, L. Parish, S. D. Cranstoun, R. Jonas, G. Baltuch, and B. Litt, "High-frequency oscillations and seizure generation in neocortical epilepsy," *Brain*, vol. 127, no. 7, pp. 1496–1506, May 2004, doi: 10.1093/brain/awh149.

[64] G. A. Worrell *et al.*, "High-frequency oscillations in human temporal lobe: simultaneous microwire and clinical macroelectrode recordings," *Brain*, vol. 131, no. 4, pp. 928–937, Feb. 2008, doi: 10.1093/brain/awn006.

[65] J. Jacobs *et al.*, "High-frequency electroencephalographic oscillations correlate with outcome of epilepsy surgery," *Annals of Neurology*, vol. 67, no. 2, pp. 209–220, Feb. 2010, doi: 10.1002/ana.21847.

[66] P. Perucca, F. Dubeau, and J. Gotman, "Intracranial electroencephalographic seizure-onset patterns: effect of underlying pathology," *Brain*, vol. 137, no. 1, pp. 183–196, Oct. 2013, doi: 10.1093/brain/awt299.

[67] N. Roehri *et al.*, "High-frequency oscillations are not better biomarkers of epileptogenic tissues than spikes," *Annals of Neurology*, vol. 83, no. 1, pp. 84–97, Jan. 2018, doi: 10.1002/ana.25124.

[68] P. N. Modur, S. Zhang, and T. W. Vitaz, "Ictal high-frequency oscillations in neocortical epilepsy: implications for seizure localization and surgical resection," *Epilepsia*, vol. 52, no. 10, pp. 1792–1801, Jul. 2011, doi: 10.1111/j.1528-1167.2011.03165.x.

[69] A. Ochi *et al.*, "Dynamic Changes of Ictal High-Frequency Oscillations in Neocortical Epilepsy: Using Multiple Band Frequency Analysis," *Epilepsia*, vol. 48, no. 2, pp. 286–296, Feb. 2007, doi: 10.1111/j.1528-1167.2007.00923.x.

[70] H. Fujiwara *et al.*, "Resection of ictal high-frequency oscillations leads to favorable surgical outcome in pediatric epilepsy," *Epilepsia*, vol. 53, no. 9, pp. 1607–1617, Aug. 2012, doi: 10.1111/j.1528-1167.2012.03629.x.

[71] K. J. Friston, C. D. Frith, P. F. Liddle, and R. S. J. Frackowiak, "Functional Connectivity: The Principal-Component Analysis of Large (PET) Data Sets," *Journal of Cerebral Blood Flow & Metabolism*, vol. 13, no. 1, pp. 5–14, Jan. 1993, doi: 10.1038/jcbfm.1993.4.

[72] J. J. Bear, K. E. Chapman, and J. R. Tregellas, "The epileptic network and cognition: What functional connectivity is teaching us about the childhood epilepsies," *Epilepsia*, vol. 60, no. 8, pp. 1491–1507, Jun. 2019, doi: 10.1111/epi.16098.

[73] P. van Mierlo *et al.*, "Functional brain connectivity from EEG in epilepsy: Seizure prediction and epileptogenic focus localization," *Progress in Neurobiology*, vol. 121, pp. 19–35, Oct. 2014, doi: 10.1016/j.pneurobio.2014.06.004.

[74] L. Corona, E. Tamilia, J. R. Madsen, S. M. Stufflebeam, P. L. Pearl, and C. Papadelis, "Mapping Functional Connectivity of Epileptogenic Networks through Virtual Implantation," submitted for publication.

[75] J.-P. Lachaux, E. Rodriguez, J. Martinerie, and F. J. Varela, "Measuring phase synchrony in brain signals," *Human Brain Mapping*, vol. 8, no. 4, pp. 194–208, 1999, doi: 3.0.co;2-c">10.1002/(sici)1097-0193(1999)8:4<194::aid-hbm4>3.0.co;2-c.

[76] National Institute of Health, "RePORT," *report.nih.gov*, Feb. 24, 2020. https://report.nih.gov/funding/categorical-spending#/.

[77] W. J. Koroshetz, "Interagency Collaborative to Accelerate Research on Epilepsy (ICARE)," *National Institute of Neurological Disorders and Stroke*, Apr. 26, 2019. https://www.ninds.nih.gov/sites/default/files/2019_icare_draft.v5_nindsupdate_wk_0_508c.pdf.

[78] S. Dumanis, "Epilepsy Research at the National Institutes of Health," *Epilepsy Foundation*, Apr. 12, 2017. https://www.epilepsy.com/article/2017/4/epilepsy-research-national-institutes-health.

[79] Interagency Collaborative to Advance Research in Epilepsy, "Reports and Publications," *icarerp.nih.gov*, May 15, 2020. https://icarerp.nih.gov/reports-and-publications (accessed Apr. 29, 2021).

[80] M. Hassan and F. Wendling, "Electroencephalography Source Connectivity: Aiming for High Resolution of Brain Networks in Time and Space," *IEEE Signal Processing Magazine*, vol. 35, no. 3, pp. 81–96, May 2018, doi: 10.1109/msp.2017.2777518.

[81] A. Zamm, S. Debener, A.-K. R. Bauer, M. G. Bleichner, A. P. Demos, and C. Palmer, "Amplitude envelope correlations measure synchronous cortical oscillations in performing musicians," *Annals of the New York Academy of Sciences*, vol. 1423, no. 1, pp. 251–263, May 2018, doi: 10.1111/nyas.13738.

[82] F. Mormann, K. Lehnertz, P. David, and C. E. Elger, "Mean phase coherence as a measure for phase synchronization and its application to the EEG of epilepsy patients," *Physica D: Nonlinear Phenomena*, vol. 144, no. 3–4, pp. 358–369, Oct. 2000, doi: 10.1016/s0167-2789(00)00087-7.

[83] S. Aydore, D. Pantazis, and R. M. Leahy, "A note on the phase locking value and its properties," *NeuroImage*, vol. 74, pp. 231–244, Jul. 2013, doi: 10.1016/j.neuroimage.2013.02.008.

[84] H. Shahabi *et al.*, "Tutorial 28: Connectivity," *Brainstorm*, Mar. 05, 2021. https://neuroimage.usc.edu/brainstorm/Tutorials/Connectivity (accessed Apr. 05, 2021).

[85] G. Pellegrino *et al.*, "Eslicarbazepine Acetate Modulates EEG Activity and Connectivity in Focal Epilepsy," *Frontiers in Neurology*, vol. 9, Dec. 2018, doi: 10.3389/fneur.2018.01054.

[86] G. Pellegrino *et al.*, "Bilateral Transcranial Direct Current Stimulation Reshapes Resting-State Brain Networks: A Magnetoencephalography Assessment," *Neural Plasticity*, vol. 2018, pp. 1–10, 2018, doi: 10.1155/2018/2782804.

[87] J.-P. Lachaux, E. Rodriguez, J. Martinerie, and F. J. Varela, "Measuring phase synchrony in brain signals," *Human Brain Mapping*, vol. 8, no. 4, pp. 194–208, 1999, doi: 3.0.co;2-c">10.1002/(sici)1097-0193(1999)8:4<194::aid-hbm4>3.0.co;2-c.

[88] J. F. Hipp, D. J. Hawellek, M. Corbetta, M. Siegel, and A. K. Engel, "Large-scale cortical correlation structure of spontaneous oscillatory activity," *Nature Neuroscience*, vol. 15, no. 6, pp. 884–890, May 2012, doi: 10.1038/nn.3101.

[89] L. Corona, "New Methods to Map the Epileptogenic Brain Networks in Children with Epilepsy: Computing the Functional Connectivity of the Epileptic Brain via 'Virtual' Intracranial Sensors", M.S. Thesis, Dept. Biomedical Engineering, Università Campus Bio-Medico di Roma, Rome, Italy, 2020.

[90] F. Tadel, S. Baillet, J. C. Mosher, D. Pantazis, and R. M. Leahy, "Brainstorm: A User-Friendly Application for MEG/EEG Analysis," *Computational Intelligence and Neuroscience*, vol. 2011, pp. 1–13, Apr. 2011, doi: 10.1155/2011/879716.

[91] A. H. Hawasli, S. K. Bandt, R. E. Hogan, N. Werner, and E. C. Leuthardt, "Laser Ablation as Treatment Strategy for Medically Refractory Dominant Insular Epilepsy: Therapeutic and Functional Considerations," *Stereotactic and Functional Neurosurgery*, vol. 92, no. 6, pp. 397–404, 2014, doi: 10.1159/000366001.

[92] J. G. Thomas, G. Rao, Y. Kew, and S. S. Prabhu, "Laser interstitial thermal therapy for newly diagnosed and recurrent glioblastoma," *Neurosurgical Focus*, vol. 41, no. 4, p. E12, Oct. 2016, doi: 10.3171/2016.7.focus16234.

[93] S. Shimamoto, C. Wu, and M. R. Sperling, "Laser interstitial thermal therapy in drug-resistant epilepsy," *Current Opinion in Neurology*, vol. 32, no. 2, pp. 237–245, Apr. 2019, doi: 10.1097/wco.0000000000000662.

[94] J. Y. Kang *et al.*, "Laser interstitial thermal therapy for medically intractable mesial temporal lobe epilepsy," *Epilepsia*, vol. 57, no. 2, pp. 325–334, Dec. 2015, doi: 10.1111/epi.13284.

[95] P. Landazuri *et al.*, "A prospective multicenter study of laser ablation for drug resistant epilepsy – One year outcomes," *Epilepsy Research*, vol. 167, no. , p. 106473, Nov. 2020, doi: 10.1016/j.eplepsyres.2020.106473.

[96] L. Douw *et al.*, "'Functional Connectivity' Is a Sensitive Predictor of Epilepsy Diagnosis after the First Seizure," *PLoS ONE*, vol. 5, no. 5, p. e10839, May 2010, doi: 10.1371/journal.pone.0010839.

[97] W. Staljanssens *et al.*, "EEG source connectivity to localize the seizure onset zone in patients with drug resistant epilepsy," *NeuroImage: Clinical*, vol. 16, pp. 689–698, 2017, doi: 10.1016/j.nicl.2017.09.011.

[98] S. P. Burns *et al.*, "Network dynamics of the brain and influence of the epileptic seizure onset zone," *Proceedings of the National Academy of Sciences*, vol. 111, no. 49, pp. E5321–E5330, Nov. 2014, doi: 10.1073/pnas.1401752111.

[99] A. R. Antony *et al.*, "Functional Connectivity Estimated from Intracranial EEG Predicts Surgical Outcome in Intractable Temporal Lobe Epilepsy," *PLoS ONE*, vol. 8, no. 10, p. e77916, Oct. 2013, doi: 10.1371/journal.pone.0077916.

[100] A. W. C. Yuen, M. R. Keezer, and J. W. Sander, "Epilepsy is a neurological and a systemic disorder," *Epilepsy & Behavior*, vol. 78, pp. 57–61, Jan. 2018, doi: 10.1016/j.yebeh.2017.10.010.

[101] T. Blauwblomme, P. Jiruska, and G. Huberfeld, "Mechanisms of Ictogenesis," *International Review of Neurobiology*, vol. 114, pp. 155–185, 2014, doi: 10.1016/b978-0-12-418693-4.00007-8.

[102] H. Kubova, K. Lukasiuk, and A. Pitkänen, "New Insight on the Mechanisms of Epileptogenesis in the Developing Brain," *Pediatric Epilepsy Surgery*, vol. 39, pp. 3–44, Nov. 2012, doi: 10.1007/978-3-7091-1360-8_1.

[103] A. Pitkänen, K. Lukasiuk, F. E. Dudek, and K. J. Staley, "Epileptogenesis," *Cold Spring Harbor Perspectives in Medicine*, vol. 5, no. 10, p. a022822, Sep. 2015, doi: 10.1101/cshperspect.a022822.

[104] S. Jahromi *et al.*, "Mapping Propagation of Interictal Spikes, Ripples, and Fast Ripples in Intracranial EEG of Children with Refractory Epilepsy", submitted for publication.

[105] M. A. G. Matarrese *et al.*, "Electric Source Imaging on Intracranial EEG Localizes Spatiotemporal Propagation of Interictal Spikes in Children with Epilepsy", submitted for publication.